RARE EARTH ELEMENTS IN THE WHITESTONE ANORTHOSITE

RARE EARTH ELEMENTS

IN

THE WHITESTONE ANORTHOSITE

By

JAMES FRANKLIN BARKER, B. Sc.

A Thesis

Submitted to the School of Graduate Studies

in Partial Fulfilment of the Requirements

for the Degree

Master of Science

McMaster University

May, 1972

MASTER OF SCIENCE (1972)
(Geology)

McMASTER UNIVERSITY
Hamilton, Ontario.

TITLE: Rare Earth Elements in the Whitestone Anorthosite

AUTHOR: James Franklin Barker, B. Sc. (McMaster University)

SUPERVISORS: Professor R.H. McNutt and Professor J.H. Crocket

NUMBER OF PAGES: xi, 93

ABSTRACT

An analytical procedure is adopted to determine eight rare earth elements in the Whitestone anorthosite, its constituent minerals, and the surrounding metamorphic rocks. Chondrite-normalized rare earth fractionation trends display the rare earth data.

Distinctive rare earth fractionation trends for anorthosites of different origins are not expected to be found. The anorthosite rare earth fractionation trends reflect the crystal-chemically controlled uptake of rare earths by the mineral phases present, so the rare earth fractionation trends of the plagioclase, clinopyroxene, hornblende and garnet are stressed. The rare earth data are consistent with plagioclase and clinopyroxene being primary phases, and hornblende and garnet being the products of autometamorphism involving the primary phases and a residual, Fe-Ti, volatile-rich fluid phase.

The country rock-anorthosite relationship is not elucidated by this rare earth study, except the suggestion that rare earths have been supplied to the metasomatic envelope from the anorthosite or a late stage, residual fluid phase associated with the anorthosite.

The theories of anorthosite origin and their application to the Whitestone anorthosite are discussed in light of rare earth information and previous field and petrologic work. The most probable modes of origin of the Whitestone anorthosite are:

1. early fractional crystallization and accumulation of a plagioclase-rich rock from a dioritic (possibly contaminated) magma, partial melting and intrusion of the anorthosite into its present geological

setting.

2. crystallization of a gabbroic anorthosite magma formed by partial fusion of amphibolite,

3. disruption (with partial melting) of a layered-type anorthosite and subsequent injection of this anorthosite into its present surroundings.

ACKNOWLEDGEMENTS

I appreciate the support give to me by my supervisors, Drs. R.H. McNutt and J.H. Crocket, throughout this work. Special thanks must go to may wife, Gayle, for her secretarial services and understanding.

TABLE OF CONTENTS

LIST OF TABLES

LIST OF FIGURES

LIST OF MAPS

CHAPTER 1

RARE EARTH ELEMENTS AND THE WHITESTONE ANORTHOSITE

INTRODUCTION

1-1. The Rare Earth Elements

The rare earth elements (denoted hereafter as REE, with rare earth denoted as RE) are defined as the lanthanides (Z = 57-71) and Y. The lightest member of group IIIa of the periodic table, Sc, is excluded because its chemical behavior is distinct from that of the REE (Cotton and Wilkinson, 1962). Promethium has no stable isotopes and is not found in nature (except as traces as a spontaneous fission fragment of uranium) so it is also excluded.

The REE are not really rare. Even the least abundant, Tm, is as common as bismuth and more common than such elements as As, Hg or Ag in the lithosphere. REE are well dispersed, but significant commercial concentrations are mined in Finland, Russia, Poland and the U.S. with the major RE ore minerals being monazite, $CePO_4$, bastnasite, $Ce(CO_3)F$, gadolinite, $Y_2FeBe_2(Si_2O_8)O_2$, and xenotime, YPO_4 (Pings, 1969).

Some properties of the REE important in RE geochemistry are outlined by Ahrens (1964) and Cotton and Wilkinson (1962). Although the normal oxidation state of all REE is +3, Ce^{4+} and Eu^{2+} can also be formed under natural conditions. The ionic radius of the lanthanide series decreases regularly with increasing atomic number, a phenomenon

known as the "lanthanide contraction". The ionic radius of Y^{3+} corresponds most closely to that of Dy^{3+} and Ho^{3+} (Whittaker and Muntus, 1970). The RE metals and their oxides are non-volatile. The metals are very reactive but the oxides are rather refractory.

The similarity in chemical properties of the REE, especially bothersome in attempts to separate individual elements from this group, has produced in geochemists the impression that these elements should constitute an extremely coherent group and any partial separation of one or more REE from the group in nature could indicate only very unusual conditions. Strong coherence of the REE was supported by such authors as Goldschmidt (1954), Taylor (1960), and Rankama and Sahama (1950), even though Goldschmidt and Thomassen (1924), Van Tongeren (1938), and Sahama and Vahatalo (1941) found extreme fractionation in the RE group in minerals and common igneous rocks. Recent work (mainly post 1960) has proven that REE undergo fractionation in nature, and exploitation of this fact in geochemical studies has begun.

The fractionation of these chemically similar elements in nature is expected to provide geochemists with yet another tool to unravel the complicated geological history of the earth and possibly the universe. However, the scarcity of information, concerning both the distribution of the REE and their physical-chemical behavior in rocks and minerals, is still critical. The need for experimental confirmation of many hypotheses concerning RE fractionation is particularly great.

1-2. The Whitestone Anorthosite

1-2-i. Geological Setting

The Whitestone anorthosite is a tear-shaped body (see Map 1, page 4)

exposed in McKenzie, Burpee, Hagerman, Ferguson, and McDougall Townships, just north of Parry Sound, Ontario. Surface exposure is good to excellent over the approximately 60 square mile body. Reconnaissance work by W.C. Lacy (1960) was followed by I. Mason's detailed Ph.D. study (Mason, 1969). Continual reference will be made to this latter work and the description of the geology of this area and the petrology of the anorthosite is from Mason's study.

The anorthosite intrudes amphibolites and gneisses which were already metamorphosed to upper almandine amphibolite facies, imposing both a thermal and a metasomatic aureole on these rocks. There has been no significant, or at least only mild, metamorphism affecting the region since the intrusion of the anorthosite.

1-2-ii. Petrology of the Whitestone Anorthosite

Only a brief summary of the petrologic observations and conclusions noted by Mason will be presented here. The reader is encouraged to refer to Mason's thesis for a more complete description of the petrology and for the persuasive evidence leading to the conclusions which are accepted here. This author, after a perusal of about 25 thin sections from the Whitestone anorthosite found no reason to doubt the following general statements of Mason (pages 31-32).

"1. Plagioclase is the most abundant phase in the anorthosite*

---

*Note: Anorthosite refers to an igneous rock containing > 77½% plagioclase of intermediate or calcic composition. Where emphasis is placed on the differences in modal mafic content of anorthosites, terms such as true anorthosite (< 10% modal mafic minerals) and gabbroic anorthosite (10-22½% modal mafic minerals) are used.

Map 1 The Whitestone Anorthosite - Facies and Sample Location

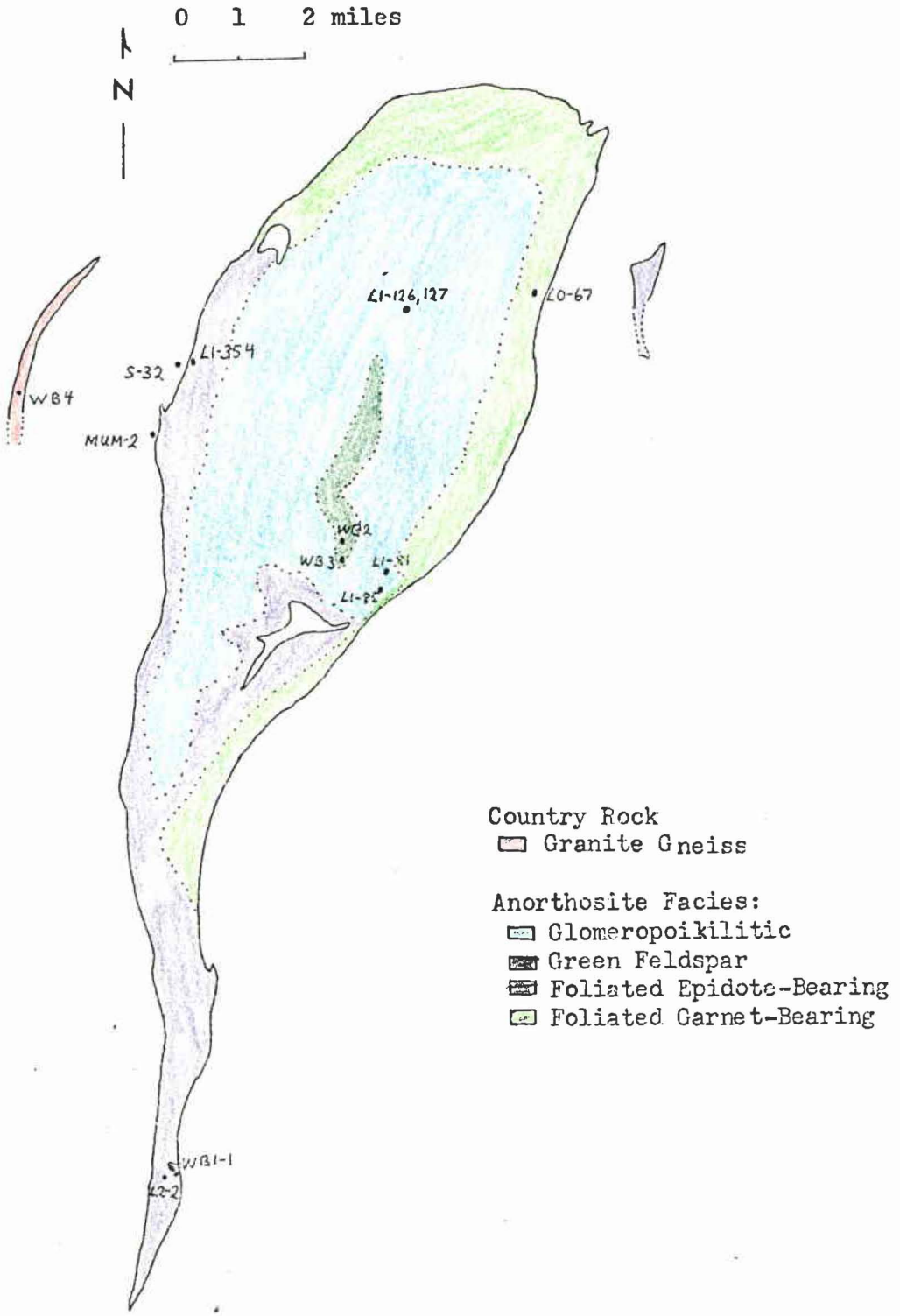

and has an average grain size of 3-5 mm. with occasional dark blue or purply grains up to 20 mm. Scapolite is common as an alteration of plagioclase.

2. The main mafic phase is clinopyroxene; uralitic amphibole is ubiquitous.

3. Apatite, oxides and associated sphene are restricted to an accessory role, except locally.

4. Garnet and epidote are restricted in distribution ...

5. The distribution of garnet and epidote is compositionally controlled."

Mason also shows that recrystallization (due to slow cooling?) is pervasive in the anorthosite specimens. The existence of an Fe-Ti, volatile rich residual fluid phase was present in the late stages of solidification.

Mason recognized two main facies - the glomeropoikilitic and the porphyritic - in the Whitestone anorthosite. Superimposed on these two primary types are three secondary facies:

1. the green feldspar facies,
2. the foliated epidote-bearing facies, and
3. the foliated garnet-bearing facies.

The distribution of these phases is shown in Map 1, page 4, and some characteristic features of these five facies are discussed below:

1. Glomeropoikilitic Facies:

This is the most abundant primary facies. "Black pyroxene occur in blotchy, sub-spherical globules or glomerules, each globule being charged with subhedral plagioclase grains, and the globules themselves are broadcast through the otherwise light grey rock in a polka-dot pattern." (Mason, page 33). As this facies grades into the foliated facies the glomerules become elongate. Re-crystallization has obscured the original exaggerated poikilitic texture.

2. Porphyritic Facies:

Mason states (page 38), "this facies is characterized by a more homogeneous distribution and, in general, a slightly higher average modal abundance of pyroxene than the glomeropoikilitic facies. ... the clinopyroxenes appear in hand specimen as distinct, rather stubby, black crystals scattered evenly throughout the rock." Igneous banding, often pyroxene enriched at the base, is occasionally seen in this facies. Blocks of disrupted banded anorthosite are also found. This facies is more restricted in distribution occuring as bands or zones within the body.

3. Green Feldspar Facies:

This facies can be considered identical to typical Whitestone anorthosite rock except for the green coloured feldspars. Both primary facies are found in the green feldspar facies. The unique green feldspars are due to "narrow, randomly oriented, yellowish or brownish veins ramifying through and around the plagioclase grains." (Mason, page 50). In this facies only, the clinopyroxene often displays a rim of secondary orthopyroxene. Also, garnet rims the mafic minerals in an unusual corona-type texture (see description of sample WB-3, Appendix A).

4. Foliated Epidote-bearing Facies:

Epidote is usually restricted to marginal, foliated rocks (see Map 1, page 4) generally free of oxide minerals. Epidote occasionally rims pyroxene.

5. Foliated Garnet-bearing Facies:

Garnet is found in some marginal, foliated rocks which contain oxide minerals but little or no epidote. Sphene is usually presented as

well. A late-stage residual Fe-Ti, volatile-rich liquid is thought to have collected in the foliated rocks, giving rise to the oxides particularly prevalent in this facies. Garnet probably has developed involving participation of oxides, pyroxene-hornblende, plagioclase and this fluid phase.

TABLE 1-1

Classification of Theories on Anorthosite Petrogenesis*

Category	Type	Author		
1	Anorthosite magma never existed as such: anorthosite is in fact a cumulate rock.	Bowen	1917	Adirondacks & General
		Balk	1931	"
		Barth	1936	Norway
		Emslie	1965	Michikumau
		Bridgewater	1967	Gardar Province
2	Massif type anorthosite crystallized from magma resulting from assimilation of country rock by 'normal' magma type	Michot P.	1960, 1955b	Egersund-Ogna Massif, Norway
		Philpotts	1966	Morin
		Kranck	1961	General
3	Massif type anorthosite crystallized directly from magma of gabbroic anorthosite composition	Buddington	1939	
			1961	Adirondacks
		Harrison	1943	S.E. Ontario
		Subramaniam	1965a	Kadavur Mass (India)
		Hargraves	1962	Allard Lake
4	Metasomatism & Anatexis	Hietanen	1956	Boehls Butte
		Berrange	1965	General
		Berg	1966	Bitterroot, Montana
		Michot J.	1961	Haland-Helleren, Norway
		Winkler & von Platen	1960	Experimental
5	Massif anorthosites are (in some cases) metamorphosed and disrupted layered intrusions	Subramaniam	1956b	Sittampundi Complex, (India)
		Windley	1967	W. Greenland

* after Mason, Table 1-2, page 9.

1-3. The Problem - The Origin of the Whitestone Anorthosite

Mason has conveniently classified the theories on anorthosite petrogenesis and his Table 1-2 (page 9) is reproduced here in Table 1-1, page 8. All five types of theories are critically discussed by Mason, pages 10 to 17, and only a brief resumé of some important points from each type is presented here.

The main point in theories of type 1 is that the anorthosite represents an initial crystal accumulate. Balk (1931) and Bowen (1917) postulate a dioritic magma from which mainly plagioclase and, intermittently, mainly mafic minerals crystallize with the residual syenite liquid forming the surrounding acidic rocks. Emslie (1965) proposes that continual separation of liquid (by volcanic activity?) from an original olivine basalt magma allowed plagioclase to continue to settle out and accumulate. Bridgewater (1967) proposes plagioclase accumulation by floatation in an already partially differentiated magma chamber. Of these authors, Emslie alone does not propose the associated acidic rocks are co-genetic.

Theories of type 2 all postulate crystallization of a primary magma modified by assimilation of crustal rock to form massif-type anorthosites.* Michot, P. (1965) and Kranck (1961) propose contamination of basaltic magma and Philpotts (1966) proposes a calc-alkaline

---

*Note: Massif-type anorthosites are "complete bodies of rock containing large domains with high modal plagioclase (> 80%) but with apparent gradation into other less plagioclase-rich domains, the whole comprising 'an anorthosite'." (Mason, page 7)

granodioritic magma derived by assimilation of crustal rocks by a dioritic magma. Philpotts postulates crystal accumulation from this magma (as in type 1) to produce the anorthosite.

The virtually complete crystallization of a gabbroic anorthosite magma characterizes type 3 theories. Buddington (1931, 1961) originated this theory for the Adirondack anorthosite and derived the gabbroic anorthosite magma by partial fusion of basalts or mantle material, both with abundant volatiles present.

Theories involving metasomatism and anatexis are listed under type 4. Michot, J. (1961) proposes partial fusion of a noritic anorthosite or leuconorite with mobilization of the ferromagnesian minerals and some plagioclase leaving behind a residuum of plagioclase - the para-anatectic anorthosite. Michot and Michot (1966) suggest that this process is active in the crust, but it does not seem clear if a pre-existing anorthosite is required or if this process accounts for a primary origin of anorthosites.

Theories of type 5 attribute some massif anorthosites to metamorphism and disruption of layered intrusions containing layered anorthosites. The application of this theory depends on the recognition of some layered-intrusive feature of the massif anorthosite.

Mason argues that the Whitestone anorthosite is "the end product of differentiation which, in turn, suggests a unique 'magma-type' derived either directly from the mantle or by fractional crystallization of a mother-magma." (page 241). This suggests Mason would best be fitted into theory type 3.

It is hoped that this work can shed some light on the question of origin of the Whitestone anorthosite. However, the scarcity of good

estimates of RE content of the mantle or possible mother magmas complicates the problem. It was decided to emphasize the mineral RE data in attempting to define the origin of the Whitestone anorthosite.

The aims of this work can be set down as follows:

1. First, an accurate yet simple analytical procedure must be adapted to determine enough REE to facilitate RE geochemical interpretations.
2. The relationship of the Whitestone anorthosite and the country rocks might be further elucidated by a study of the REE in these rocks. Of particular interest is the possibility of co-genetic relationships in the anorthosite-envelope rocks.
3. The fractionation of the REE between the mineral phases in the anorthosite are to be determined and explained if possible.
4. The RE data is to be used to indicate the more probable origins of the Whitestone anorthosite.

1-4. The Samples

Anorthosite samples collected by Mason and by this author for RE analysis were thin sectioned and Table A-1 indicates the modes of the anorthosite samples based on > 1000 points counted for each section. A brief petrographic description for all but two thin sectioned samples is compiled in Appendix A. Sample locations are indicated on Map 1, page 4.

CHAPTER 2

ANALYTICAL PROCEDURE

2-1. Sample Preparation

Samples L1-85, L1-81, LO-67, L1-126, L1-127, L2-2, L1-354 and the corresponding mineral fractions were obtained from I. Mason. The whole rock samples were already crushed to less than 200 mesh. The mineral separates were checked optically and were found to be greater than 99% pure in all cases. Each separate was crushed to less than 200 mesh with an agate mortar and pestle and stored in a glass vial.

R. Mummery, McMaster, supplied samples Mum-2 and S-32 already crushed to less than 200 mesh.

Samples WB1-1, WB2, and WB3 were collected by the author. To obtain a representative whole rock sample of each, fresh chips were broken off each with a hammer and crushed in a Spex shatterbox to less than 200 mesh. The powder was halved, recombined 10 times to ensure homogeneity, and stored in a carton.

To obtain pure mineral fractions of each sample, anorther portion was crushed in the Spex shatterbox and the 100 to 200 mesh fraction collected. The Franz Isodynamic separator and heavy liquid separations using tetrabromoethane, methyl iodide, and acetone were employed to separate the constituent minerals. Plagioclase plus scapolite was separated to greater than 99.8% purity, while pyroxene, hornblende, biotite, and garnet fractions contained up to 5% impuritities (mainly other mafic minerals) when checked optically. Each separated

phase was crushed to less than 200 mesh using an agate mortar and pestle and stored in a glass vial.

2-2. Standard and Carrier Preparation

A standard solution containing the approximate expected concentration of REE was made up by taking into solution accurately weighed individual RE oxides (spec-pure, Rare Earth Products, Limited). The solution was made up to exactly 1000 ml. in a volumetric flask as 2.0 M HCl and its density calculated using the weight of oxides added and the density of 2.0 M HCl given in The Handbook of Physics and Chemistry. The standard solution contained the following concentrations of REE:

REE	conc. (μgm REE/gm solution)
Y	16.69
La	6.68
Ce	6.43
Pr	11.26
Nd	6.43
Sm	4.27
Eu	3.01
Gd	3.65
Tb	4.83
Dy	2.56
Ho	5.19
Er	2.75
Tm	4.49
Yb	4.81
Lu	3.09

A similar procedure was used to make up a carrier solution containing from 0.1 to 1 mg./ml. of each RE oxide. Another carrier solution containing accurately weighed La_2O_3 and Yb_2O_3 (about 10 mg/ml. each) was also made up in dilute acid. One ml. of each carrier solution was used in processing each sample and standard after irradiation. This provided a carrier for each RE , and also a large excess of La and Yb whose yields could be determined by re-irradiation with negligible background due to other RE nuclides.

2-3. Irradiation

About 100 mg. of sample powder was accurately weighed into a labelled 4 mm. O.D. fused silica ampoule and sealed by fusing the open end. About 0.1 ml. of standard solution was accurately weighed into a similar ampoule and slowly evaporated to dryness at 70-80°C. in a heating oven before fusing. The silica tubing had been previously cleaned by boiling in aqua regia and washing with distilled water.

Six samples and one standard were irradiated simultaneously in an aluminum can in a high flux position in the McMaster Nuclear Reactor (nominal neutron flux of 1.5×10^{13} neutrons/cm.^{2}/sec.). Irradiation times of 2 to 4 days were used followed by 3 to 5 days cooling before chemical processing.

2-4. Post-Irradiation Chemistry

The complete chemical procedure for both samples and standards is given in Appendix B. Briefly, following digestion with HF and $HClO_4$ precipitation of the rare earths with carriers as hydroxides and then fluorides (3 times repeated) was used to separate them from virtually all other elements. Scandium, however, must be further removed by solvent extraction in the system 8.0 M HCl and tri-butyl phosphate. The standard was processed only to obtain the same counting geometry as the samples; consequently, no fluoride precipitation or extraction was carried out. Six samples and one standard required 8 to 10 hours to process in this manner.

2-5. Counting

The nuclides used and some of the pertinent information for the eight rare earth elements determined in this work are listed in

Table 2-1, page 16. The rare earth fractions were gamma counted at three different times after irradiation to optimize determination of nuclides of various half-lives as follows:

Time after irradiation ends	Nuclides determined
5 days	^{140}La, ^{153}Sm
10 -12 days	^{175}Yb, ^{177}Lu
5 weeks	^{141}Ce, ^{152}Eu, ^{160}Tb, ^{170}Tm, ^{169}Yb

Counting errors were minimized by counting standard and samples in volumetric flasks as homogeneous solutions. Each flask was located in the same position relative to the detector to obtain identical counting geometries for samples and standards. Dead time corrections were unnecessary as dead time did not exceed 20% in any case.

The gamma spectrum was calibrated with 84 KeV ^{170}Tm, 320 KeV ^{51}Cr, and 662 KeV ^{137}Cs. RE nuclide peaks were located and printed out with approximately 10 channels on either side of the peak to obtain a background.

2-6. Counting Equipment

Gamma counting was carried out with a hybrid system consisting of:

i) a Canberra 130 gm. Ge(Li) solid state detector crystal with an 8 cm^2 active area

ii) high voltage supply (1900 V.) for the crystal (Canberra)

iii) low noise FET preamplifier (Canberra)

iv) spectroscopy amplifier (Canberra)

Table 2-1: Nuclear Properties of Nuclides and Photopeaks Used in RE Determination[1].

Element	Target Nuclide	Product Nuclide (n,γ reaction) and half life	Production Factor[2]	Photopeaks Used (KeV)	Interferences and Comments
La	La^{139}	La^{140} (40.2 hr)	13	490	
Ce	Ce^{140}	Ce^{141} (32.5 d)	0.04	145	The 145 KeV peak of Yb^{175} (4.19 d) is negligibly small because of its extremely low intensity
Sm	Sm^{152}	Sm^{153} (46.8 hr)	71	103	The 103 KeV of Gd^{153} (236 d) is extremely small (< 1% of Sm^{153} peak at 103 KeV)
Eu	Eu^{151}	Eu^{152} (12.7 yr)	1.2	343	
Tb	Tb^{159}	Tb^{160} (72.4 d)	1.8	298	
Tm	Tm^{169}	Tm^{170} (129 d)	2.5	84	The contribution of the 87 KeV peak of Tb^{160} must be subtracted mathematically before Tm can be determined (usually 30-50% of total peak)
Yb	Yb^{168}	Yb^{169} (31 d)	60	177	
	Yb^{174}	Yb^{175} (4.19 d)	3.6	396	
Lu	Lu^{176}	Lu^{177} (6.71 d)	20	208	The peak can be differentiated from the 216 KeV peak of Tb^{160} and from the 198 KeV peak of Yb^{169} but the selection of a suitable background is difficult

1. from Table of Isotopes, Lederer et al (1967)

2. Production Factor = cross section of target (barns) x $\frac{\text{time of irradiation (60hr)}}{\text{half-life of product}}$ x $\frac{1}{100 \text{ barns}}$

d = days hr = hours yr = years

v) 1600 channel RIDL pulse height analyzer

vi) Hewlett-Packard display oscilloscope and teletype printer.

The amplifier was adjusted so that the energy range 60 to 700 KeV was counted. The energy resolution for the Cr^{51} peak at 320 KeV was 4.5 KeV (full width at half maximum).

2-7. Calculations

2-7-i. Activity Calculations

The half-peak area method was used to calculate gamma ray activities. For each peak, the spectrum was integrated over the full width at half maximum and the average background was subtracted. Background was determined from the average activity of 5 channels on both sides of the peak. This background is mainly due to the Compton plateaus from higher energy gammas. Occasionally small gamma peaks at the margins of counted peaks made it necessary to choose channels removed from the counted peak as suitable background.

Activities were recalculated to a common time to compare samples and standards.

2-7-ii. Element Concentration Calculation

By comparing the activity of the elements in the sample with that in the standards and correcting for the variable chemical yields, the element concentrations were obtained.

The following relation was used in the calculation:

$$C = c \cdot \frac{M}{W} \cdot \frac{A}{a} \cdot Y$$

where: c = concentration in ppm of the element in the standard

M = weight of standard irradiated

W = weight of sample irradiated

A = activity of the element in the sample

a = activity of the element in the standard

Y = yield of the element in the sample relative to the yield in the standard

C = element concentration in the sample in ppm.

CHAPTER 3

RESULTS

3-1. Precision, Accuracy, and Comparison with Other Work

To evaluate the precision of this method the coefficient of variation (C.V.), calculated as the percent standard deviation divided by the mean value, is presented for all replicate analyses. Replicates were analyzed in separate irradiations. Also, analyses of the standard rocks W-1, BCR-1, and AGV-1 are presented in Table 3-1, page 20, along with the standard deviation, S, and the coefficient of variation. These standards were selected as their rare earth concentrations were similar to those expected in the anorthosite and country rocks, and the precisions reported are representative of those in the rest of this work.

The precision ranges of the rare earths determined were:

C.V. (%)	
5 - 15	La, Eu, Lu
10 - 25	Sm, Tb
15 - 35	Ce, Tm Yb.

It is pertinent to note the correspondence of the precision ranges above with the usual peak/background ratio for the gamma photopeaks used in this study:

Peak/Background (approx.)	Element
>4/1	La, Eu, Tb
2/1 - 4/1	Lu, Sm, Tm
< 2/1	Ce, Yb.

Table 3-1: Precision of REE Determinations in Standard Rocks W-1, BCR-1 and AGV-1

Element	W-1 (5 analyses)			BCR-1 (3 analyses) Split 72 Position 9			AGV-1 (3 analyses) Split 103 Position 14		
	conc. ppm	S	C.V. %	conc. ppm	S	C.V. %	conc. ppm	S	C.V. %
La	10.7	1.05	9.7	18.7	2.1	11.2	28.7	2.8	9.8
Ce	19.4	2.42	12.5	27.4	6.2	22.6	43.9	6.1	13.9
Sm	3.03	0.89	29.4	4.4	0.47	10.7	4.02	0.86	21.4
Eu	1.24	0.22	17.7	2.49	0.034	1.4	1.21	0.10	8.3
Tb	0.60	0.10	16.7	1.12	0.043	3.8	0.68	0.18	26.5
Tm	0.33	0.10	30.3	0.64	0.070	9.2	0.35	0.068	19.4
Yb	1.87	0.55	29.4	3.0	1.1	36.7	1.64	0.16	10.3
Lu	0.37	0.036	10.3	0.66	0.033	5.0	0.38	0.014	3.7

S = standard deviation

C.V. = coefficient of variation (%) = S/mean value x 100%

The precision appears to be limited mainly by the statistical uncertainties involved in determination of these peaks. The peaks with higher peak/background ratios lead to more precise determinations. As the sensitivity limit is approached (peak/background ratio $\rightarrow$ 1) the precision decreases. Also, the mathematical correction necessary to determine Tm abundances would decrease the precision of Tm analyses greatly. Because background acitivity depends on the variable matrix of the sample, it is impossible to define a sensitivity limit to cover all analyses. Suffice it to say that those elements whose precision is consistently poor (Ce, Tm, Yb) are close to the sensitivity limits.

The accuracy of the method is more difficult to assess. The best standard available with a RE concentration in the expected range for anorthosites ($\lesssim$ REE = 10 - 100 ppm) is the standard rock W-1. Many reputable RE analyses are found in the literature for W-1. Although W-1 does not represent a chemically similar material to the anorthosite, its correspondence to expected anorthosite RE abundances is good. Two other U.S.G.S. standard rocks, BCR-1 and AGV-1, are considered useful in ascertaining the accuracy of RE determinations for country rock. The country rock is expected to contain $\lesssim$ REE = 100 - 500 ppm and both BCR-1 and AGV-1 fall in this range. Again the overall chemical similarity of these standard rocks and the expected country rock (gneisses, amphibolites) is not good, but the similarity in RE concentrations makes them acceptable for the estimation of accuracy of this method.

If the most precise values are also taken as the most accurate as suggested by Smales (1971), then the analysis of W-1 and BCR-1 by mass spectrometer isotope dilution (Philpotts and Schnetzler, 1970) will

be taken as the most accurate values. However, only half the REE of interest are determined by the isotope dilution technique. The agreement of the analyses of Philpotts and Schnetzler with those of Haskin and Gehl (1963) for W-1 is within 5%, so the later analysis will be compared to this work. The differences between Haskin and Gehl's values and those of this study are expressed as a percent of the value found in this work (in Table 3-2, page 23). Positive differences indicate this work is the higher, and vice-versa. In BCR-1, the agreement of Haskin et al (1970) with Philpotts and Schnetzler (1970) is only within 15%. A comparison of RE data for BCR-1 from this work with that of Haskin et al shows much poorer agreement (see Table 3-2, page 23) than for W-1. Negative differences are noted for all REE save Eu and Lu.

Table 3-2 shows that for W-1, the REE determined in this work fall inside the range of values from other analyses except for Sm (low in this work) and Lu (high in this work). The generally larger range of values for REE determined in the standards BCR-1 and AGV-1, and the poorer agreement of this work with other analyses in these standards, could indicate sample inhomogeneity is important in standards BCR-1 and AGV-1. This problem has been suggested in BCR-1 by Rey et al (1970) and Haskin et al (1970). However, the very low determinations of Ce and Sm in BCR-1 and AGV-1 in this work must be noted.

The accuracy of this method is expected to be within the limits of precision for all anorthosite and anorthosite mineral RE analyses. For the samples of higher RE content (i.e. country rock samples) the accuracy is expected to be within the limits of precision for all REE, except Ce and Sm which are probably reported too low in this work.

Table 3-2: Comparison of Some Analyses of the Standard Rocks W-1, BCR-1 and AGV-1

Element	W-1							
	Tomura et al[1] (1965)	Higuchi et al[2] (1970)	Towell et al[3] (1965a)	Taylor[4] (1965)	Schnetzler, Philpotts[5] (1970)	Haskin, Gehl[6] (1963)	This work Avg. of 5 Analyses	Comparison %
La	13.9	12.2	9.3	13.5		11.7	10.7	-9.4
Ce	24	26.3	15.1	18	23.4	24	19.4	-24
Pr								
Nd	21	18.2	20.2	11	15.1	15		
Sm	3.78	3.77	3.46	3.3	3.76	3.8	3.03	-24
Eu	1.04	1.25	1.29	0.95	1.112	1.09	1.24	+12
Gd	3.4	3.84		3.0	4.03	4.2		
Tb	0.60	0.665	0.81	0.66		0.75	0.60	-40
Dy		3.67	4.4	2.6	3.95			
Ho		0.801	0.855	0.78				

cont...

Method of Analysis:
1,2 - NAA following group separation of REE
3,6 - NAA following individual RE separation by ion exchange
4 - Spark source mass spectrometry
5 - Isotope dilution mass spectrometry

Table 3-2 (cont'd)

W-1

Element	Tomura et al[1] (1965)	Higuchi et al[2] (1970)	Towell et al[3] (1965a)	Taylor[4] (1965)	Schnetzler, Philpotts[5] (1970)	Haskin, Gehl[6] (1963)	This work Avg. of 5 Analyses	Comparison %
Er				1.8	2.30			
Tm	0.30	0.336	0.332	0.31		0.36	0.33	-10
Yb	1.9	2.06	2.23	1.57	2.08	2.1	1.87	-12
Lu	0.35	0.353	0.348		0.31	0.33	0.37	+11

	BCR-1					AGV-1			
Element	Higuchi et al[2] (1970)	Philpotts, Schnetzler[5] (1970)	Haskin et al[7] (1970)	This work (Avg. of 3)	Comparison %	Gordon et al[8] (1968)	Green et al[9] (1969)	Higuchi et al[2] (1970)	This Work (Avg. of 3)
La	23.8		25.2	18.7	-34	33	32	44	28.7
Ce	62.2	53.9	54.2	27.4	-98	57	56	83	43.9
Pr									
Nd	28	32.1	30.5			47	30.5	43	
Sm	7.3	7.44	7.23	4.4	-63	5.4	4.95	6.69	4.02

Table 3-2 cont'd.

	BCR-1					AGV-1			
Element	Higuchi et al[2] (1970)	Philpotts, Schnetzler[5] (1970)	Haskin et al[7] (1970)	This work (Avg. of 3)	Comparison %	Gordon et al[8] (1968)	Green et al[9] (1969)	Higuchi et al[2] (1970)	This Work (avg. of 3)
Eu	2.39	1.92	1.97	2.49	+20	1.55	1.17	1.97	1.21
Gd	7.0	6.47	8.02				7.2	5.76	
Tb	1.17	1.0	1.15	1.12	-2.7	0.77	0.62	0.72	0.68
Dy	6.25	6.36	6.55					3.74	
Ho			1.34						
Er		3.58	3.51						
Tm				0.64		0.6			
Yb	3.58	3.38	3.48	3.04	-14	1.6	1.45	1.68	1.64
Lu	0.55	0.536	0.526	0.66	+20	0.37	0.18	0.257	0.38

Method of Analysis:
7 - NAA following individual RE separation by ion exchange
8 - INAA with interference corrections
9 - NAA following group separation of REE

3-2. Potential Sources of Error

Some general factors leading to error in activation analysis along with steps taken to alleviate them should be mentioned. Variation in neutron flux for samples and standards was minimized by irradiating samples and standards together in close proximity. Differences in conditions of counting the rare earth fractions were reduced by counting homogeneous solutions in similar flasks and in the same position relative to the detector.

Other factors pertinent to this work are considered in more detail below:

3-2-i. Standard Preparation

The systematic differences between RE concentrations measured in this work and those measured by other analysts suggest an error in standard preparation. It is felt that errors in weighing the oxides used are not significant. Another source of error could be the non-stoikiometry of the RE oxides. For example, the cerium oxide was reported as CeO_2. If some Ce_2O_3 was present, the results reported here would be too low. No standardization, either by comparison with an exact standard or by EDTA titration, was attempted so the accuracy of the standard is unknown. Some standardization now seems necessary in any future work.

3-2-ii. Sample Inhomogeneity

Poor precision in RE analyses of rocks and minerals has been traced to the problem of sample inhomogeneity (Haskin and Gehl, 1963, Schmitt et al, 1963). Rey et al (1970) state "the higher light rare earth abundances [in a second analysis of BCR-1] are probably attri-

butable to varying amounts of accessory mineral in the two analyzed fractions."

The rare earths show a strong tendency to form rare earth minerals in granitic and pegmatitic rocks (Vlasov, K.A., 1966), but many minerals found only in trace quantities in basic rocks tend to concentrate rare earths also. Examples include apatite and zircon (Nagasawa, 1970) and ilmenite and sphene (Smith, 1970). Thus the inhomogeneous distribution of these phases could lead to poor reproducibility or precision of whole rock rare earth determinations. As Fritze and Robertson (1969) point out, REE incorporated in the more homogeneous major phases could give a minimum value of rare earth content, and any minor rare earth concentrating phase, if not homogeneously distributed in the powdered samples, would lead to imprecise higher values.

The effect of sample inhomogeneity in this work is not considered serious. Where possible, large volumes of sample were crushed to < 200 mesh, divided and recombined to obtain a representative sample. The largest sample practicable (usually 100-150 mg.) was irradiated. Most anorthosite samples (for example LO-67, L1-127, L1-81) contain traces of rare earth concentrating phases (apatite, sphene, carbonate) but these showed about the same precision as sample L1-126 which was free of these phases. Lack of definite indications of sample inhomogeneity with respect to rare earth elements, through systematic precision variations, probably precludes the consideration of inhomogeneity as a source of major errors.

3-2-iii. Shielding Effects

The very large thermal cross section of many rare earths, especially Dy, Eu, and Sm, make the consideration of shielding effects necessary.

Michelsen and Steinnes (1969) found that the shielding of REE in the activation analysis of apatite and iron ore (Eu concentrations of 52-59 ppm) was not significant. For the present samples, having much lower RE concentrations, the shielding effects must be negligible.

Michelsen and Steinnes also considered the self-shielding effects of Eu. A linear relationship was found between known and determined concentrations up to 200 ppm Eu, indicating that self-shielding of Eu was not significant up to 200 ppm Eu. It appears that self-shielding can be ignored in this work as a source of error.

Shielding effects, then, can be considered negligible in the concentrations found in this work. However, what effect will concentrations of rare earths in trace-accessory phases have? Fritze and Robertson (1969) speculated that low determinations might result from shielding effects. Mosen et al (1961) estimate up to 20% flux reduction and a similar error due to Eu shielding if the rare earths are concentrated as oxide spheres. The rare earth concentrating trace-accessory phases observed (apatite, sphene, carbonates) probably contain about the same concentration as Michelsen and Steinnes' analyzed apatite and would not have serious shielding effects.

In regard to shielding effects in standards, Plumb and Lewis (1955) recommend that thin target standards be used to reduce the shielding effects. Evaporated standards provide the thin geometry required. Mosen et al (1961) found less than 8% difference in effective neutron flux between thin rare earth targets (foil or evaporated solutions) and rare earth targets encased in 5 g. chondrite mockups. Since much smaller quantities of rock are used here, the shielding in the sample is probably

negligible, and the difference in effective neutron flux (between samples and standards) is probably less than 1%.

3-2-iv. Interfering Nuclear Reactions

The effects of interfering nuclear reactions are dependent upon the composition of the sample and the nuclear properties of its constituents. Three types of interfering reactions are considered:

1. fast neutron induced reactions which yield the same nuclide as the thermal induced reactions. ex. $^{152}Eu\ (n_f, p)\ ^{153}Sm$ interfering with $^{152}Sm\ (n, \gamma)\ ^{153}Sm$.

2. fission of heavy elements - U fission producing ^{140}La, ^{141}Ce and ^{153}Sm.

3. activation products decaying to the stable parent isotope of the nuclide of interest - e.g. $^{139}La\ (n, \gamma)\ ^{140}La \xrightarrow{\beta^-} ^{140}Ce\ (n, \gamma)\ ^{141}Ce$.

1. To estimate the effects of fast neutron reactions, the fast neutron component is estimated at 20% of the total neutron flux (probably the upper limit). The most favoured interfering reactions are:

$$^{144}Nd\ (n, \alpha)\ ^{141}Ce \quad \text{and} \quad ^{153}Eu\ (n,p)\ ^{153}Sm.$$

Ratios of Nd/Ce and Eu/Sm of 10^4 are required to produce a 1% contribution from the fast neutron reactions to the ^{141}Ce and ^{153}Sm produced by thermal neutrons, so (n,p) and (n, α) reactions will not affect this work.

2. Schmitt et al (1963) considered the problem of U fission as a source of ^{140}La, ^{141}Ce, and ^{153}Sm. Using their calculations, ratios of U/La = 50, U/Ce = 10, and U/Sm = 50 are required to produce a 1% addition to the (n, γ) produced nuclides. These ratios are considerably higher than those in most igneous rocks (W-1 < 1/3, G-1 < 1/10 for U/Sm for example), so U fission is disregarded as a source of error in this work.

3. The most serious intering reactions of the third type would be:

$$^{139}\text{La}\ (n,\gamma)\ ^{140}\text{La}\ldots\ ^{\beta^-}\ ^{140}\text{Ce}\ (n,\gamma)\ ^{141}\text{Ce}.$$

Following the calculations of Kant et al (1956), it can be shown that, for 1% of the expected ^{141}Ce activity to originate as ^{139}La, the ratio of La/Ce must be about 30/1. This is far higher than observed La/Ce ratios, and this process can also be neglected.

Thus, interfering nuclear reactions can be neglected as sources of error in this RE analysis. Shielding effects and sample inhomogeneity probably have only minor importance, but both are difficult to evaluate precisely. The general coincidence of precision with peak/background ratios would indicate a major contribution to poor precision from statistically poor counting conditions of some gamma peaks.

3-3. Analytical Results

The results of the RE activation analyses are presented in Tables 3-3 and 3-4. The number of replicate analyses are shown under the sample number, and the coefficient of variation (C.V.) is calculated where applicable.

Major element analyses for some of these samples can be found in Mason (1969).

Certain samples were analyzed for Sr content by R.H. McNutt employing isotope dilution techniques with a Sr^{86} enriched spike. The Sr values are preliminary as spike calibration is required. However, the Sr values are expected to be within 10% of true values and such accuracy is sufficient for this work. XRF analyses by P. Wojack were employed in Sr analyses of plagioclase fractions and these values have an accuracy within 10%. The Sr values are given in Table 3-5.

Table 3-3: Whole Rock Rare Earth Abundances (ppm)

Element	WB-3 (5)	C.V.	WB-2 (4)	C.V.	L1-126 (2)	C.V.	L1-127 (3)	C.V.
La	3.17	15	2.60	8.3	3.85	4.6	4.01	6.6
Ce	3.8	30	10.1		4.6		8.1	
Sm	1.61	10	0.82	9.1	0.86	9.8	1.52	5.9
Eu	1.17	8.1	0.72	23	1.04	6.8	0.92	7.6
Tb	0.28	7.2	0.48		0.13		0.33	0.0
Tm	0.24	23					0.22	15.7
Yb	1.12	5.4	0.60		0.45		1.01	4.1
Lu	0.22		0.16				0.13	8.4

Element	L1-81 (1)	C.V.	L1-85 (4)	C.V.	LO-67 (4)	C.V.
La	2.90		2.12	9.4	5.68	8.9
Ce	4.0		5.84	12	8.7	15
Sm	1.38		1.18	11	2.38	6.9
Eu	1.20		1.02	11	1.35	7.0
Tb	0.46		0.43	12	0.50	10
Tm	0.19		0.22	42	0.27	5.4
Yb	0.96		1.02	2.6	1.75	8.1
Lu	0.11		0.16	35	0.23	62

C.V. = coefficient of variation % = standard deviation/mean value x 100%

Table 3-3 cont'd: Whole Rock Rare Earth Abundances (ppm)

Element	L2-2 (1)	C.V.	WB1-1 (3)	C.V.	L1-354 (1)	C.V.	Mum-2 (3)	C.V.
La	2.01		3.13	11	2.90		20.3	3.5
Ce	3.8		3.8		3.3		42.2	5.7
Sm	0.66		0.42	4.1	1.05		10.8	24
Eu	0.77		0.74	17	0.94		4.71	19
Tb	0.08		0.17		0.16		1.79	9.0
Tm			0.086	16	0.08		0.84	22
Yb			0.41		0.56		3.89	14
Lu			0.18				0.74	1.4

Element	S-32 (2)	C.V.	WB-4 (2)	C.V.
La	35.5	26	54.7	8.6
Ce	5.98	2.8	72.5	
Sm	8.65	12	13.8	
Eu	1.60	40	4.60	4.6
Tb	1.30	13	3.0	14
Tm			1.3	
Yb	4.30		9.5	15
Lu	0.55	58	1.54	

Table 3-4: Rare Earth Abundances (ppm) - Minerals

Element	WB-3 Plag. (2)	C.V.	WB-3 Pyx. (1)	WB-3 Gar. (1)	WB-2 Plag. (2)	C.V.
La	3.60	16	2.63	0.16	3.17	4.9
Ce	5.5				4.0	14
Sm	0.15	9.4	3.64	1.62	0.151	2.8
Eu	0.50		1.62	1.34	0.50	22
Tb	0.04		0.38	1.06	0.038	
Tm				0.86		
Yb	0.16		4.33	5.31		
Lu				0.78		

Element	WB-2 Pyx.+ Hb. (1)	WB-2 Gar. (1)	L1-127 Plag. (2)	C.V.	L1-127 Pyx. (1)
La	2.40	0.59	2.79	2.6	2.97
Ce	3.10		4.05		4.60
Sm	1.36	2.81	0.20	21	2.47
Eu	0.52	1.41	0.25	11	1.10
Tb		1.80	0.03		0.41
Tm		0.97			0.28
Yb	2.64	10.3	0.10		1.85
Lu		1.52	0.01		0.38

Table 3-4 cont'd: Rare Earth Abundances (ppm) - Minerals

Element	Ll-127 Hb. (1)	Ll-81 Plag. (3)	C.V.	Ll-81 Pyx. (1)	Ll-81 Hb. (3)	C.V.
La	2.56	2.92	8.2	2.80	2.26	14
Ce	3.20	3.33		3.19	3.9	
Sm	2.10	0.41	7.9	2.74	2.71	13
Eu	1.18	0.66	12	1.34	1.59	7.3
Tb	0.52	0.073		0.48	0.63	14
Tm	0.37			0.44	0.42	
Yb	1.90			2.0	2.22	
Lu	0.43			0.30	0.30	

Element	Ll-85 Plag. (2)	C.V.	Ll-85 Pyx. (1)	Ll-85 Hb. (1)	LO-67 Plag. (3)	C.V.
La	2.01	1.8	1.76	4.60	7.09	5.1
Ce				6.05	9.7	23
Sm	0.27	16	1.68	2.09	0.48	16
Eu	0.53		0.80	1.07	0.78	11
Tb	0.05		0.39	0.39	0.09	
Tm			0.41	0.40		
Tb			1.33	1.98		
Lu			0.31	0.40		

Table 3-4 cont'd: Rare Earth Abundances (ppm) - Minerals

Element	L0-67 Pyx. (1)	L0-67 Gar. (1)	L2-2 Plag. (1)	L2-2 Bio. (2)	C.V.
La	4.59	0.58	0.39	3.55	13
Ce	8.0			1.98	
Sm	5.61	2.80	0.062	0.125	9
Eu	2.17	1.21	0.32	0.081	7
Tb	0.60	1.20	0.008	.002	
Tm	0.43	1.20			
Yb	2.11	6.70		0.48	
Lu	0.30	0.99	0.01		

Element	WB1-1 Plag. (3)	C.V.	WB1-1 Hb. (1)
La	0.61	3.8	4.80
Ce			7.9
Sm	0.047	17	1.98
Eu	0.57	9	0.89
Tb	0.01		6.36
Tm			0.34
Yb			1.70
Lu			0.26

Plag. = plagioclase Hb. = hornblende Bio.= biotite

Pyx. = pyroxene Gar. = garnet

Table 3-5: Sr Analyses of Some Mineral Concentrates - Whitestone Anorthosite

No.	L2-2		L0-67		L1-127	
Mineral Phase	plag.	biotite	plag.	pyroxene	plag.	pyroxene
Sr (ppm)	704	35.7	732	24	1043	33

CHAPTER 4

DISCUSSION

4-1. Presentation of Data

It is difficult to present a complete, yet not ponderous, picture of the results of multi-element analyses for numerous samples. Subjectivity, usually based upon the interpretations being made, enters into the presentation of findings. This is evident in rare earth geochemistry.

The tabulation of ratios of individual REE or groups of REE points out some specific facts but neglects other, less important (?) ones. Balashov (1963), in particular, has stressed the significance of such ratios as Eu/Sm in geological processes. With the advent of NAA and the determination of 14 REE, even in material having less than ppm concentrations, the presentation of data reflected the more complete analyses. RE concentration versus atomic number plots could be used to visually and mathematically compare RE patterns effectively. The major problem was the domination by the zig-zag relation of even-odd atomic number plots referred to as the Oddo-Harkins rule. To eliminate this, the pattern could be divided into even REE and odd REE before comparison, or the single pattern could be normalized to its clarke or some other value which showed the same zig-zag pattern. To facilitate geochemical interpretations Coryell and co-workers (1963) suggested that each RE be divided by its abundance in some primitive matter - specifically the chondrites. For most materials, a much smoother pattern is obtained when the logarithm of the chondrite-normalized values of each RE is plotted against atomic number or ionic radius. This yields a plot showing the fractionation of each RE relative to the primitive

pattern.+ It must be stressed that this smoothing can be done using other normalizing values which the reader might consider better represent a primitive RE pattern or which provide a smoother trend.

In this work the results are presented graphically. The logarithm of the concentration of each RE divided by the concentration of the corresponding RE in chondrites is plotted against ionic radius (8-fold coordination) for each RE. The ionic radius, rather than the atomic number was used as ordinate since crystal-chemical interpretations will be based on ionic radius considerations. The values for the RE ionic radii are those of Whittaker and Muntus (1970) given below in Table 4-1. These are based on cation bonding with O and F only, but the covalent as well as the ionic nature of the bonds are considered so their suitability in silicate geochemistry is suggested. The curve for the change in radius along the lanthanide series is somewhat smoother and much less steep than it is according to Ahren's figures. (W and M, Fig. 1).*

The values of the REE in chondrites is taken as the average in 20 chondrites compiled by Haskin and Gehl (1963). The values of interest are found in Table 4-2.

The chondrite-normalized RE patterns for the 10 samples from the Whitestone anorthosite are grouped according to facies recognized by I. Mason, and are presented in Figure 4-1. Also, the "composite" RE pattern for this anorthosite (an average of each facies pattern) is shown.

+ Such a plot also shows the trend or pattern of fractionation of the REE. Generally each RE has a particular value of RE sample/RE chondrite or particular fractionation, and when these values are plotted against ionic radii of the REE, an overall trend or pattern of fractionation can be seen.

* A point to remember for later discussion: in 8-fold coordination the ionic radius of Ca^{2+} now corresponds best to that of Nd^{3+} rather than Sm^{3+} according to Ahren's data.

Table 4-1: Ionic Radii of the REE and Calcium

(from Whittaker and Muntus, 1970)

Element and Valence State	Ionic Radius (Å) 6-fold coordination	8-fold coordination
Ca^{2+}	1.08	1.20
La^{3+}	1.13	1.26
Ce^{3+}	1.09	1.22
Ce^{4+}	0.88	1.05
Pr^{3+}	1.08	1.22
Nd^{3+}	1.06	1.20
Sm^{3+}	1.04	1.17
Eu^{2+}	1.25	1.33
Eu^{3+}	1.03	1.15
Gd^{3+}	1.02	1.14
Tb^{3+}	1.00	1.12
Dy^{3+}	0.99	1.11
Ho^{3+}	0.98	1.10
Er^{3+}	0.97	1.08
Tm^{3+}	0.96	1.07
Yb^{3+}	0.95	1.06
Lu^{3+}	0.94	1.05
Y^{3+}	0.98	1.10

Table 4-2: Chondritic Concentrations of REE (ppm)

Element	La	Ce	Sm	Eu	Gd	Tb	Tm	Yb	Lu
Conc. (ppm)	0.30	0.84	0.21	0.074	0.32	0.058	0.033	0.17	0.031

Figure 4-2 shows the chondrite-normalized RE patterns for 5 other anorthosites.

4-2. Anorthosite Rare Earth Patterns (see Fig. 4-1, 4-2)

All the RE trends show a greater, positive fractionation (enrichment) of the lighter REE (La - Gd) than of the heavy REE (Tb - Lu, Y) compared to the chondrites. However, the dominant feature of all anorthosite RE patterns is the large, positive Eu anomaly.+ The ratio Eu/Eu^* (see note below) ranges from about 2 in the Whitestone anorthosite to about 6 in the Southern Quebec example, with the others intermediate at about 4.

The overall fractionation patterns also show some differences. The Southern Quebec and lunar anorthosites are less enriched in the light REE than the others, while the Norwegian and Southern Quebec ones are less enriched in the heavy REE. In overall trend, the Whitestone and lunar anorthosites exhibit less difference in light and heavy REE fractionation (i.e. a flatter trend). Even the steeper trends of Southern Quebec and Norwegian anorthosites have differences - the inflection of the trends of Stromfjord and Storvann anorthosites at about Tb.

These similarities and differences can be better understood after presentation of the mineral data, as crystal-chemical control of RE uptake by minerals and the abundance of these minerals accounts best for the whole rock RE fractionation trends.

+ An anomalous value of Eu in the RE fractionation pattern is one which is considerably different than would be expected from extrapolation between Sm and Gd or Tb.

Note: Eu/Eu^* where Eu is the chondrite-normalized value observed, and Eu^* is that value predicted by graphical extrapolation between the values of Sm and Tb (or Gd) and also normalized to chondrites.

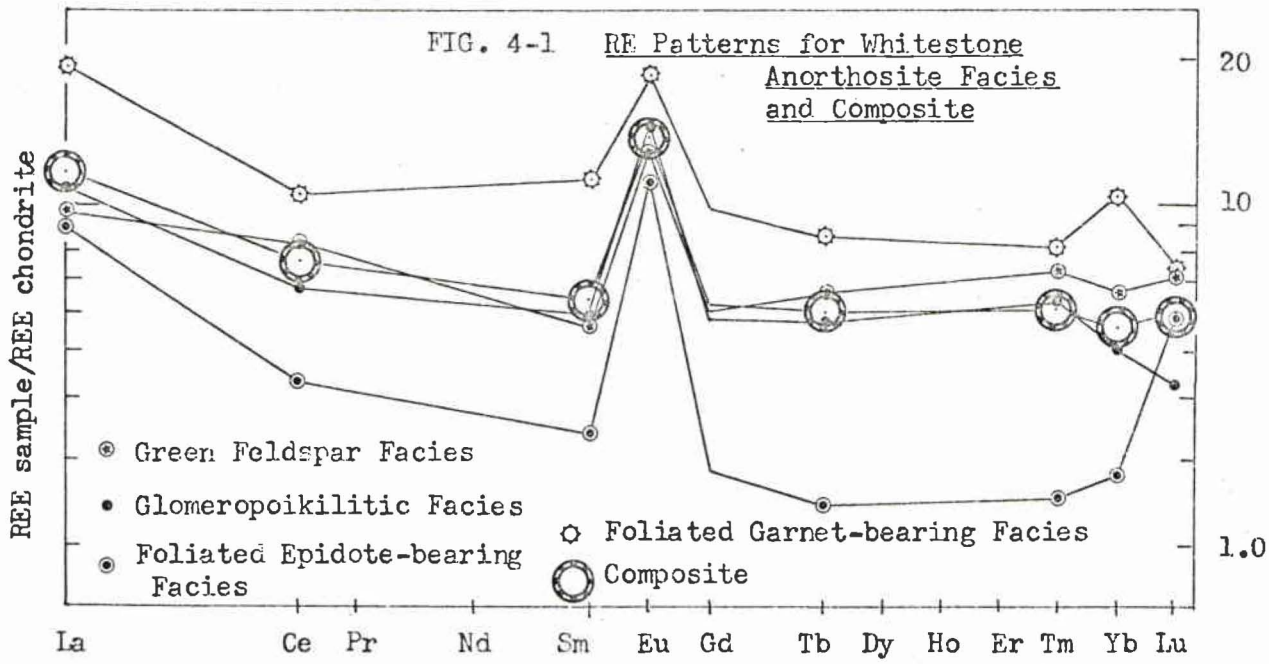

FIG. 4-1 RE Patterns for Whitestone Anorthosite Facies and Composite

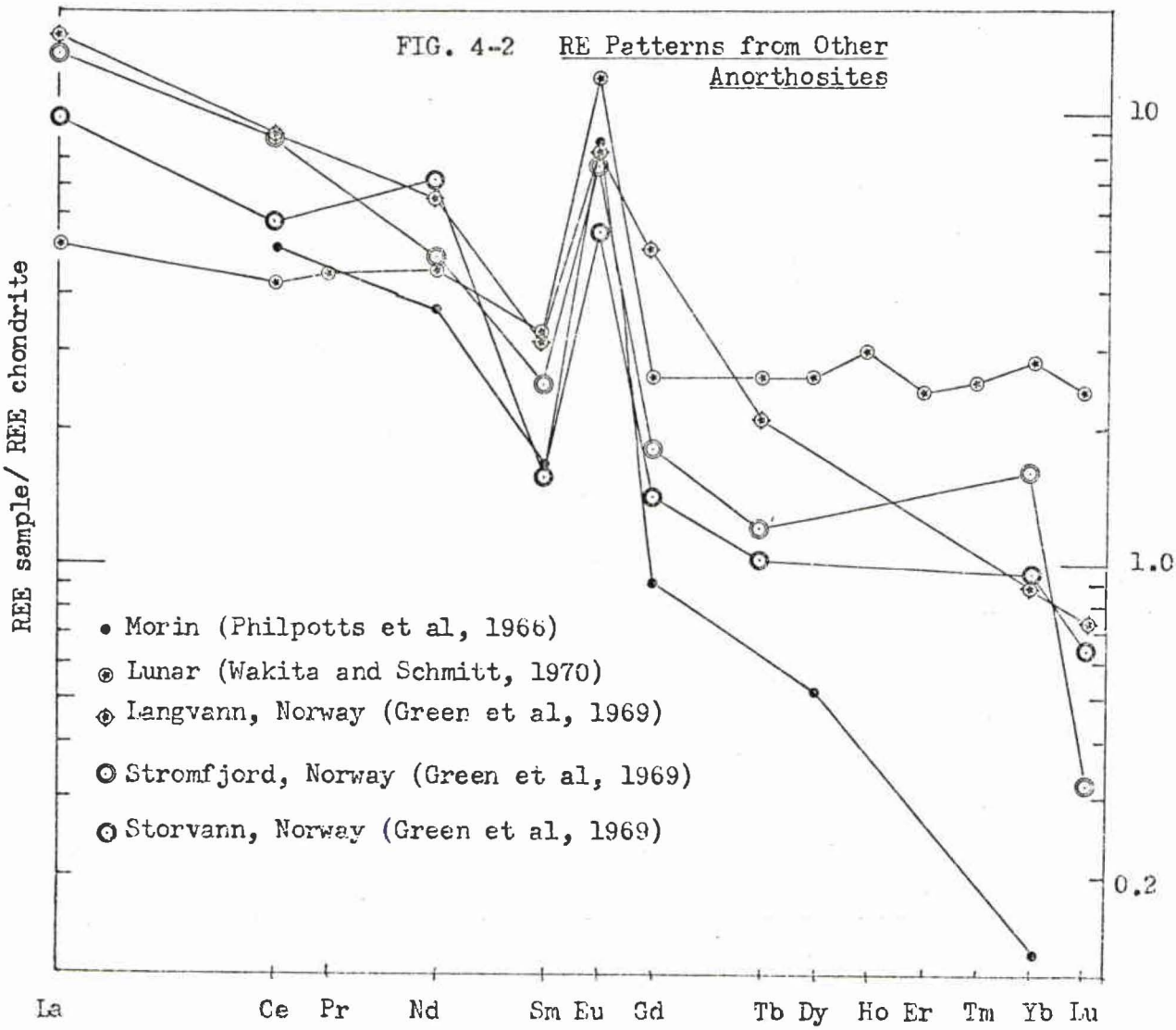

FIG. 4-2 RE Patterns from Other Anorthosites

4-3. Anorthosite Mineral RE Patterns

4-3-i. Presentation of Mineral RE Trends

The fractionation of the REE between a liquid and crystallizing phases can be represented by normalizing, element by element, the RE fractionation patterns of the mineral phases against the original liquid's RE fractionation pattern. As in chondrite normalization, the fractionation of the REE between the crystalline products relative to an original material is obtained in a smoothed, graphical form. But what was the RE content of the original liquid? Schnetzler and Philpotts (1970) took the glassy matrix of volcanics to represent original liquid. Chilled zones in layered intrusions have been considered the best available estimate of the original liquid (Frey et al, 1968 - Stillwater, Bushveld intrusions). In some plutonic rocks, the whole rock RE pattern is considered the equivalent of that in the original liquid (Towell et al, 1965). The latter case assumes that the minerals present represent complete solidification of the mother liquid with no RE loss.

In the Whitestone anorthosite, and in anorthosites generally, this last assumption is probably not applicable. The dominant poikilitic texture suggests cumulate plagioclase trapped some residual fluid from which plagioclase and pyroxene crystallized. Possibly the original liquid is better represented by the interstitial pyroxene-plagioclase, but the whole rock RE content is probably strongly biased by the large volume of cumulate plagioclase. This does not deny the possibility of an anorthositic mother liquid, in which case the whole rock - original liquid equality might hold, but rather leaves the question open. Also, the suggestion by Mason that a residual fluid phase was involved in the formation of secondary hornblende,

scapolite, garnet, etc., ("autometamorphism" - Mason) and that this liquid was expelled from the anorthosite, further weakens the assumption of whole rock-original liquid equality.

Thus, the RE concentrations in analyzed mineral are divided, element by element, by the concentration in the chondrites. Figure 4-3 shows the chondrite-normalized RE fractionation trends for both mineral and whole rock analyses of 7 Whitestone anorthosite samples. This allows immediate comparison of mineral and whole rock fractionation trends.

To discuss the crystal-chemistry of the REE and the anorthosite minerals, the fractionation trends from Figure 4-3 are grouped according to mineral phase in Figure 4-4. The consistency of fractionation trends in each phase is noted, with minor fluctuations. The magnitude of fractionation is variable, but the trends are generally parallel.

Before drawing any interpretations, a reminder of some experimental limitations seems necessary. Not all the REE were determined, and of those determined, Ce could be reported 100% low and Sm 65% low in the Whitestone anorthosite. Care must be taken not to emphasize trends strongly dependent on minor Ce and Sm differences. Error bars are not shown on the RE fractionation trends. Reference is suggested to Tables 3-3 and 3-4 for an estimate of probable errors.

4-3-ii. Plagioclase-RE Crystal-Chemistry

The RE fractionation trends of the plagioclase are grouped in Figure 4-4a. The trends are almost parallel but the overall magnitude of fractionation from the chondrite pattern is variable (ex. La enrichment varies from 1.3 to 24). The fractionation of REE in all plagioclase samples

FIG. 4-3 (a) RE Patterns for WB-3

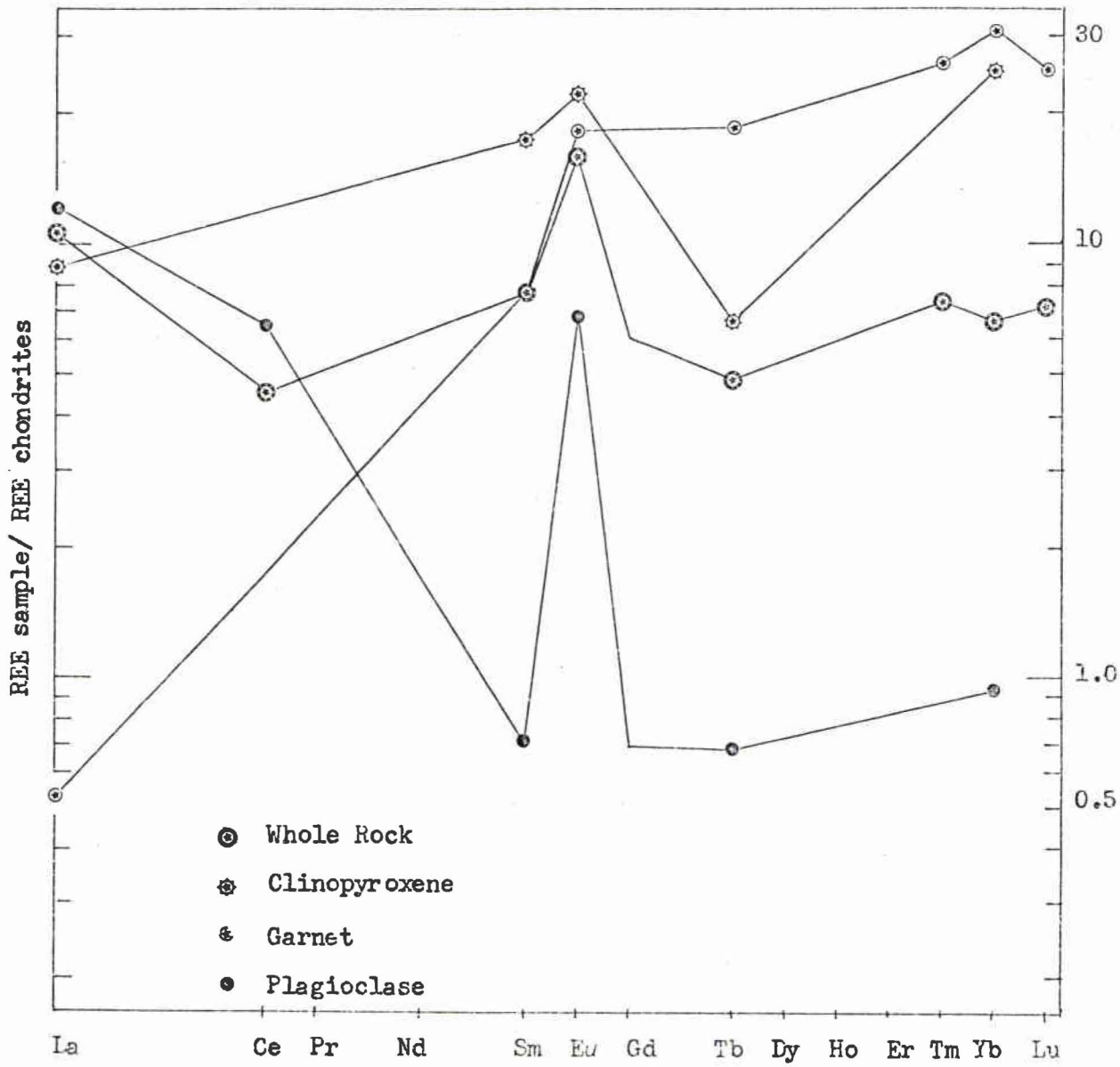

FIG. 4-3 (b) RE Patterns for WB-2

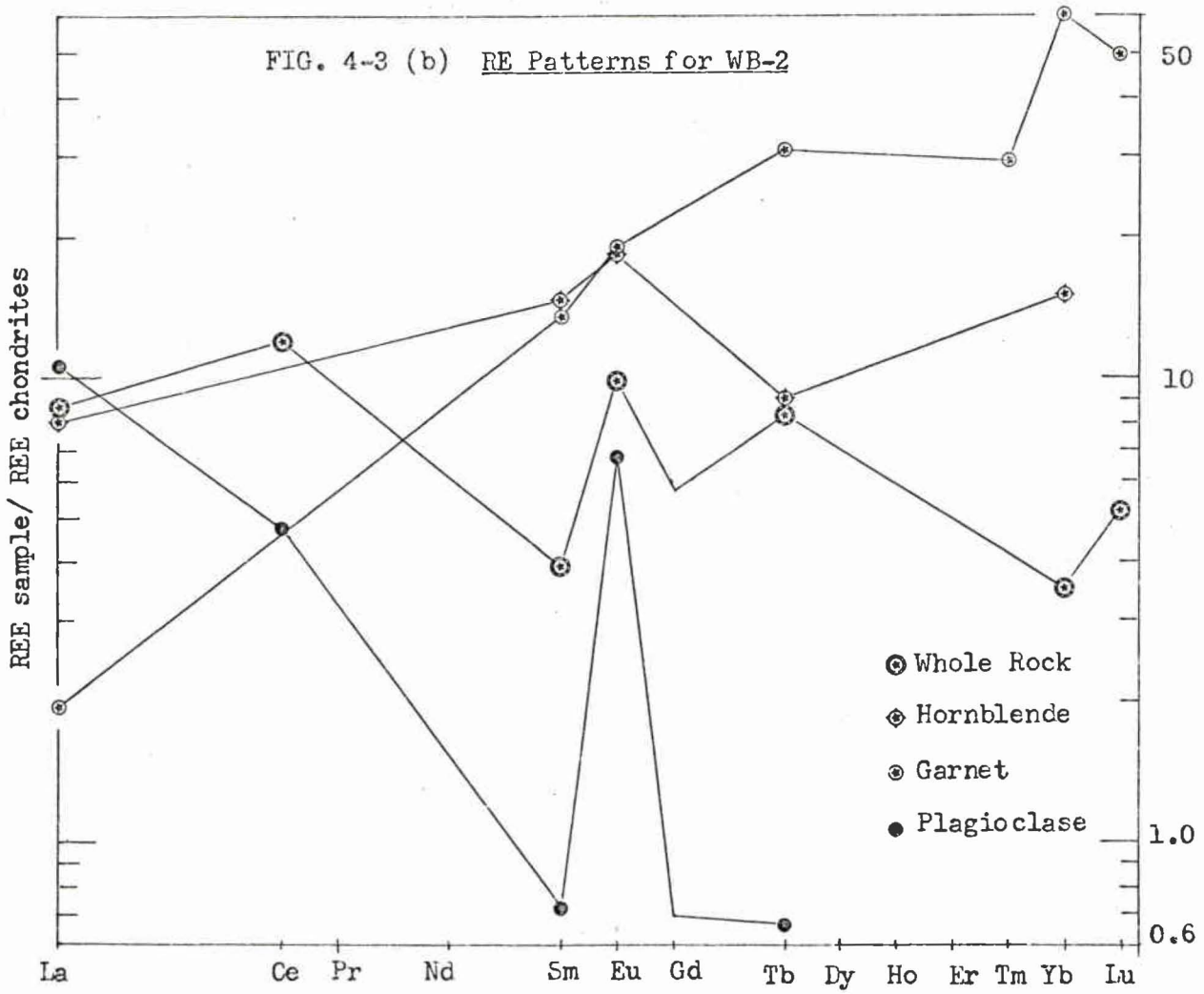

FIG. 4-3 (c) RE Patterns for L1-81

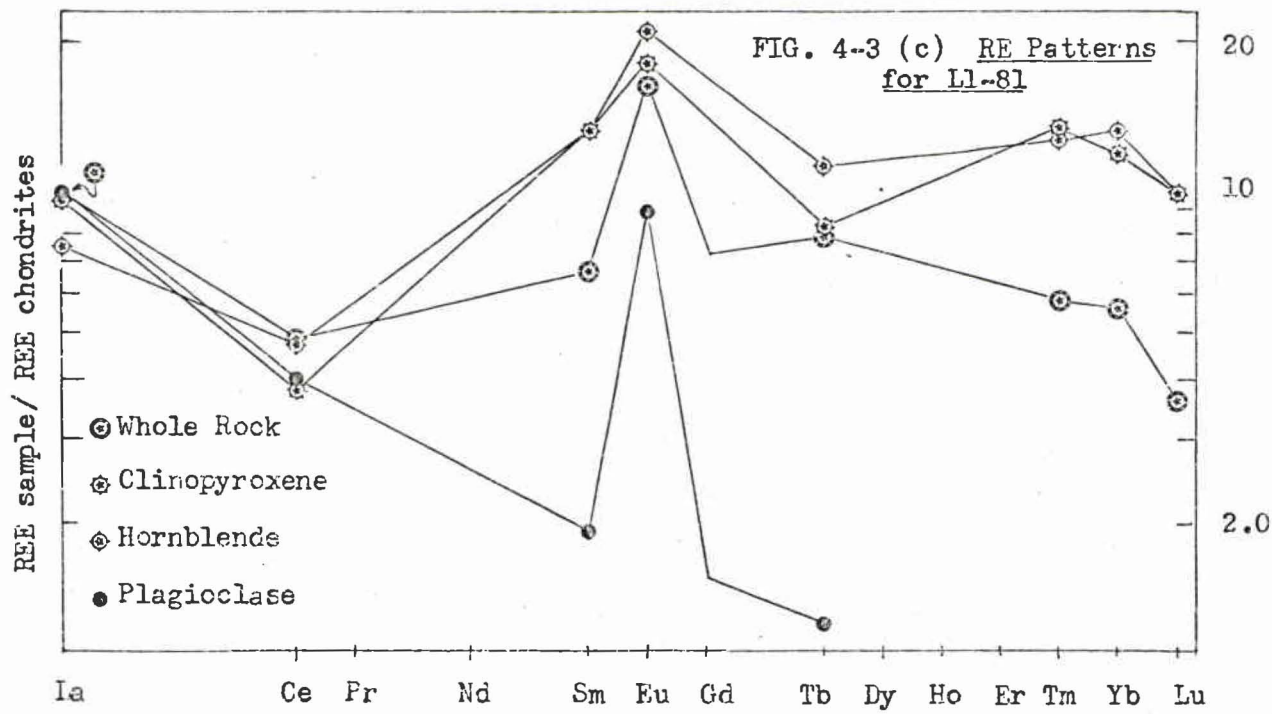

FIG. 4-3 (d) RE Patterns for Ll-85

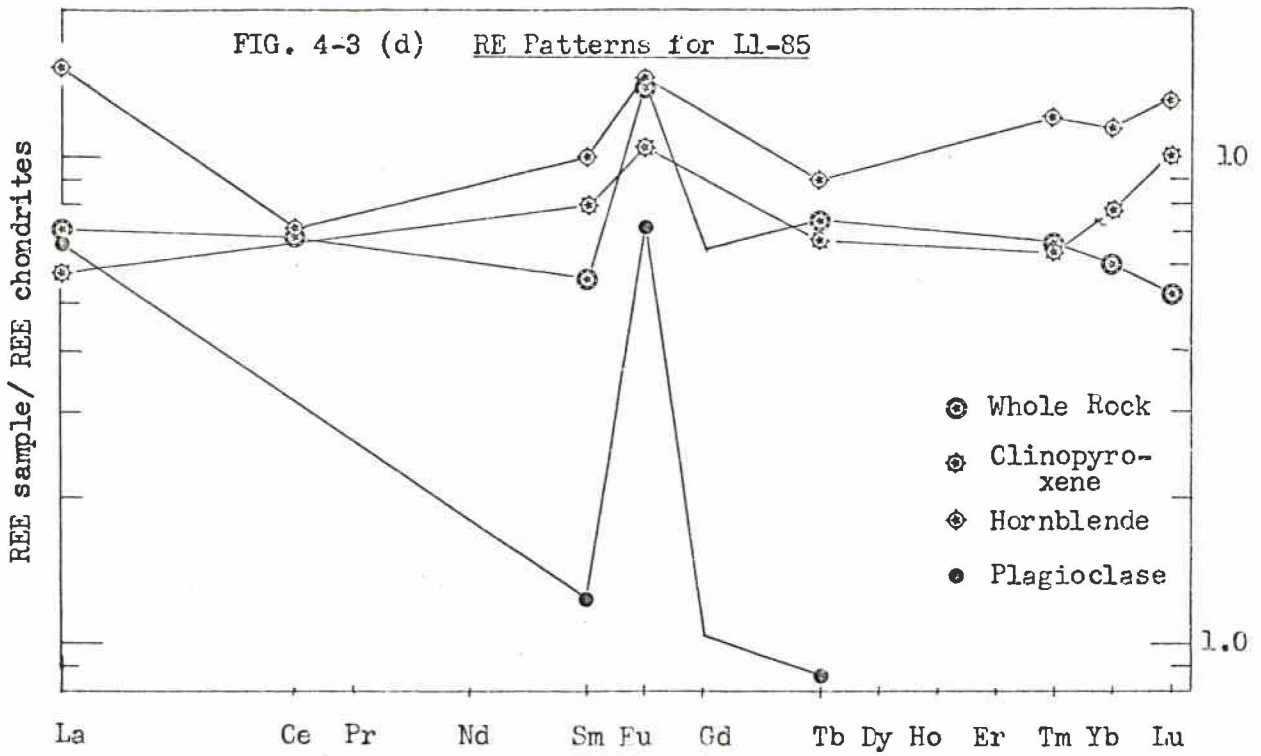

FIG. 4-3 (e) RE Patterns for Ll-127

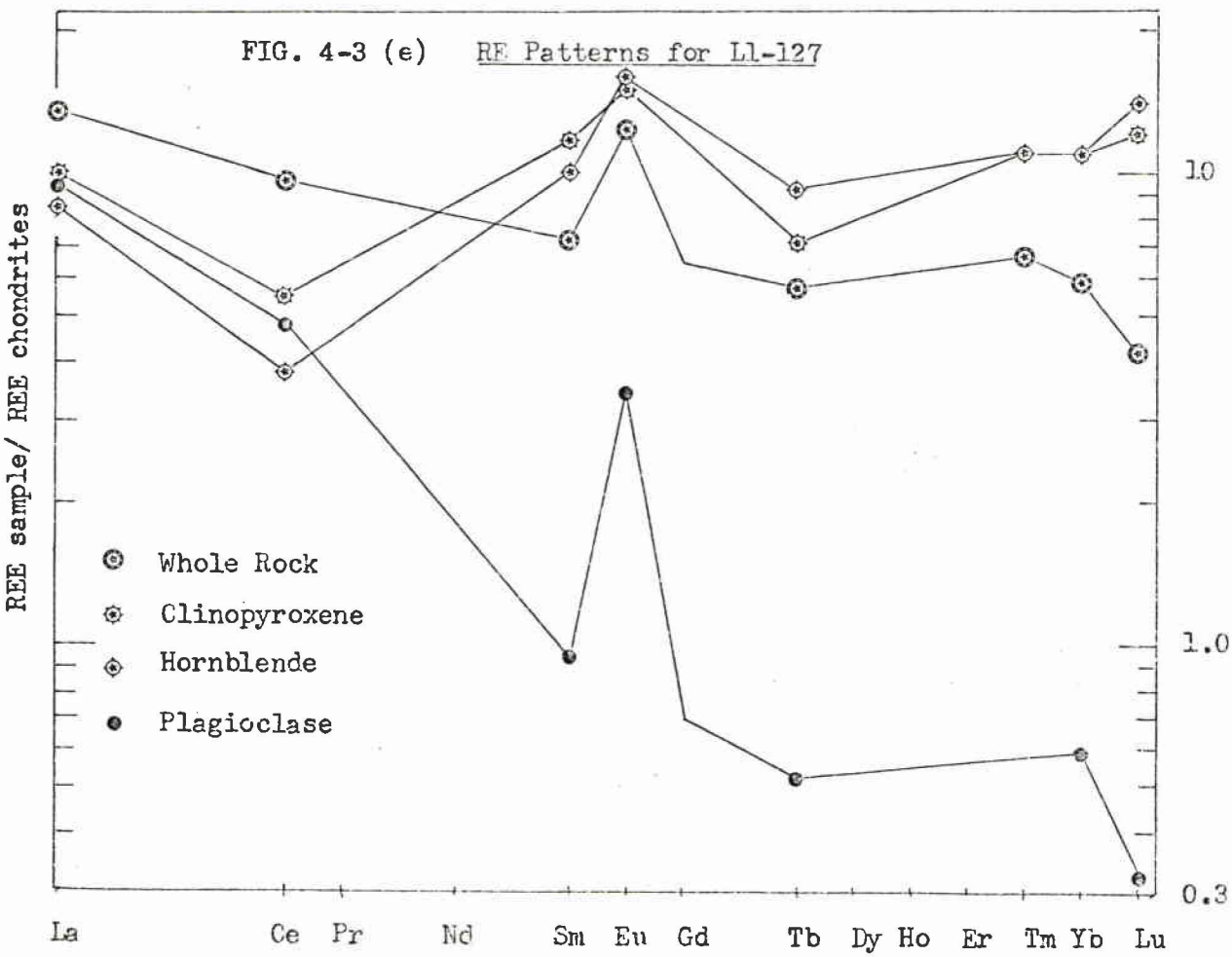

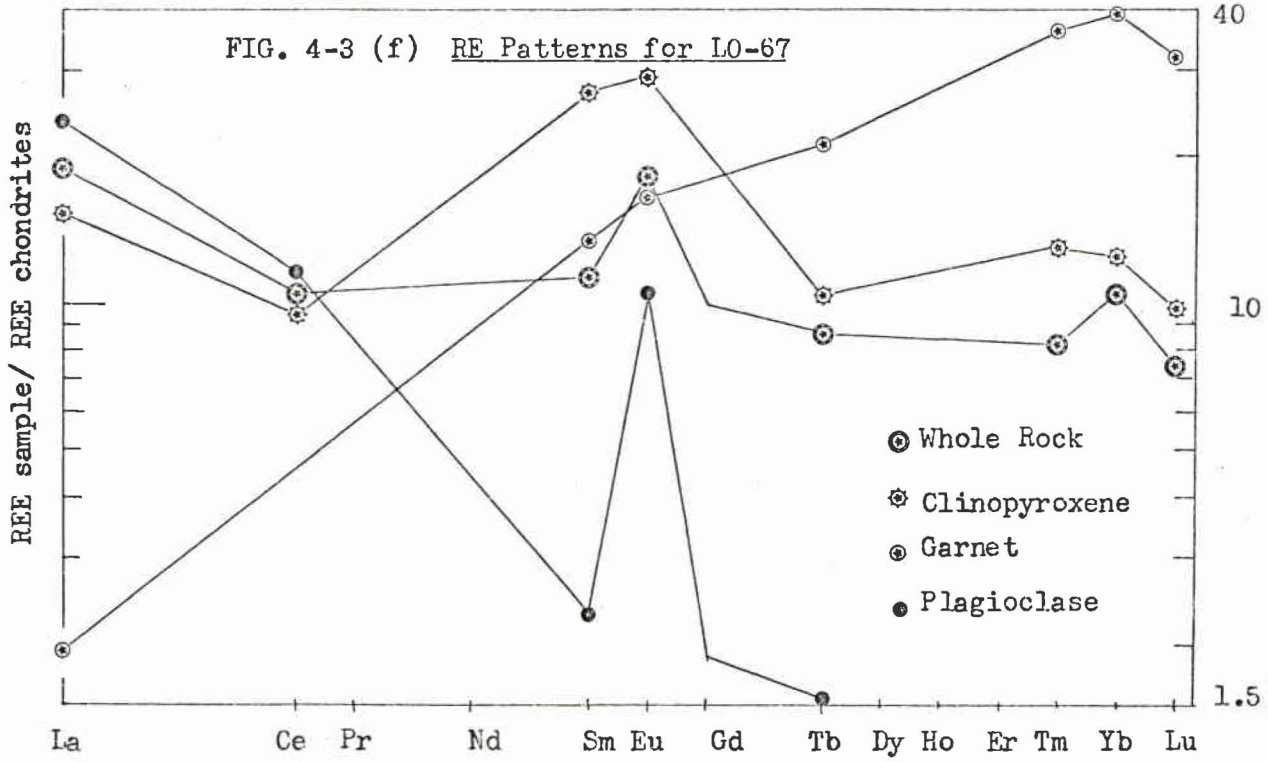

FIG. 4-3 (f) RE Patterns for LO-67

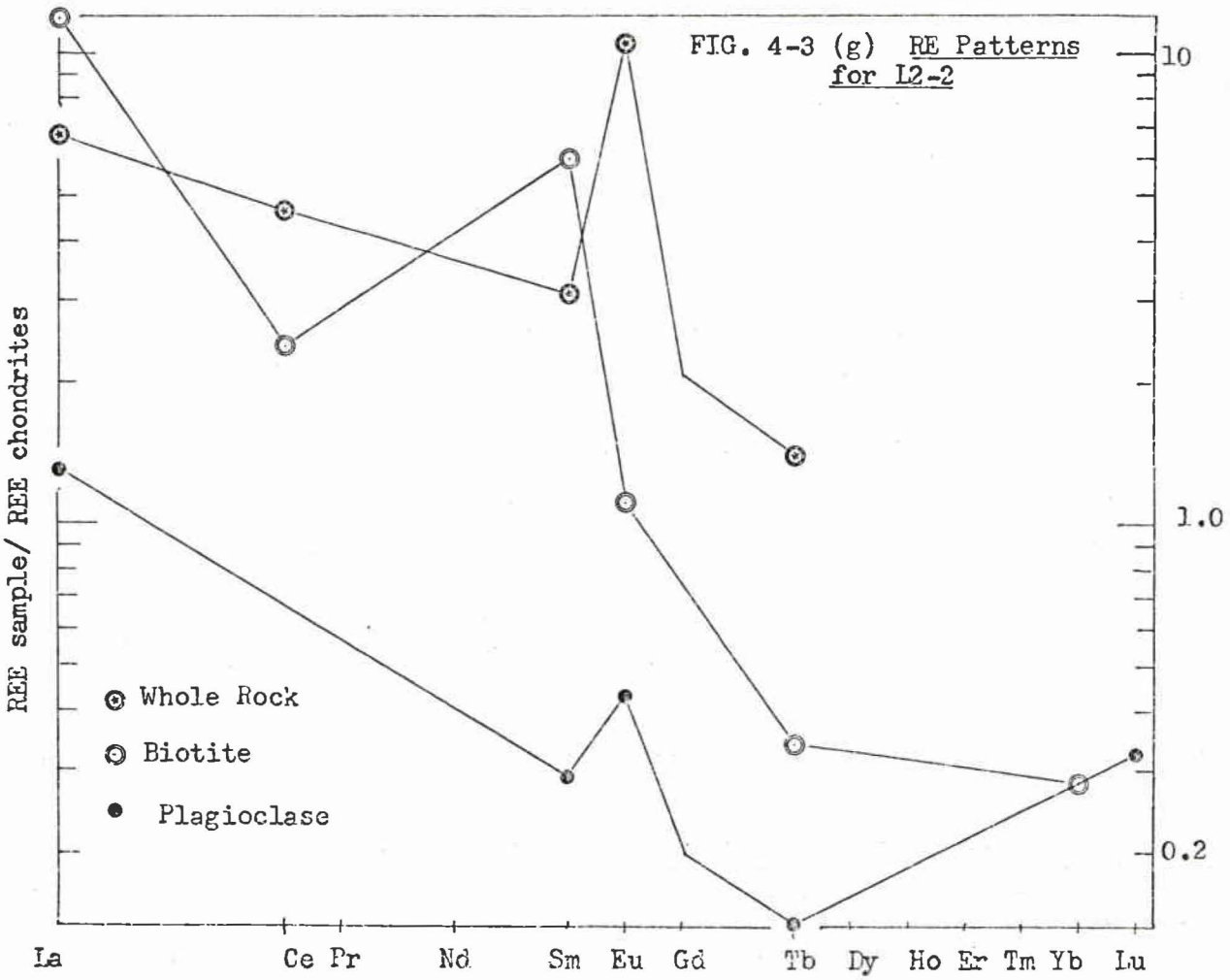

FIG. 4-3 (g) RE Patterns for L2-2

FIG. 4-4 (a) RE Trends in Plagioclase

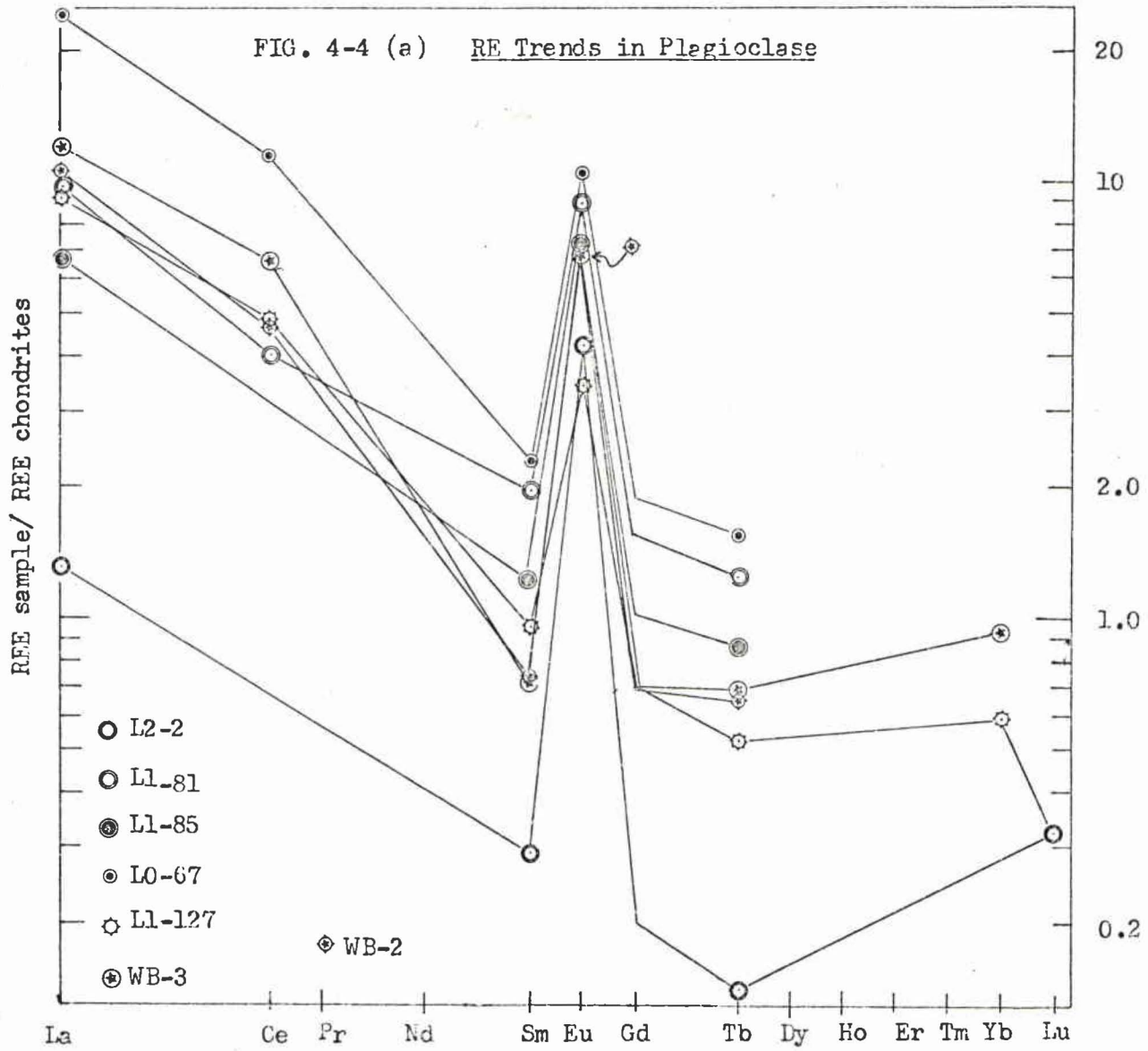

FIG. 4-4 (b) RE Trends in Clinopyroxenes

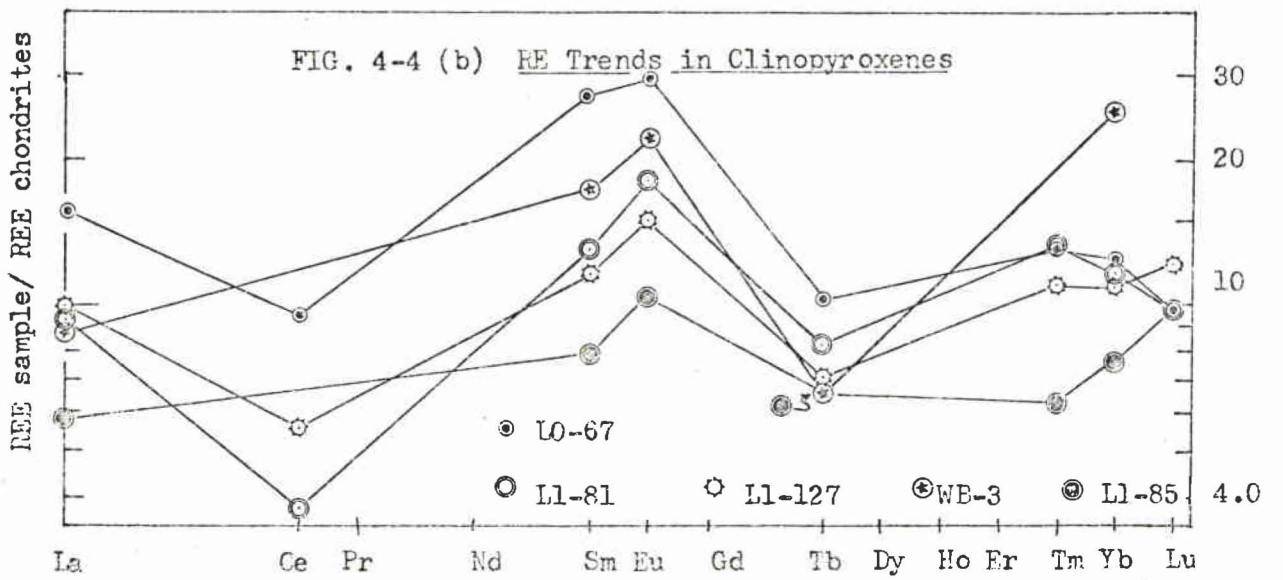

FIG. 4-4 (c) RE Trends in Hornblendes

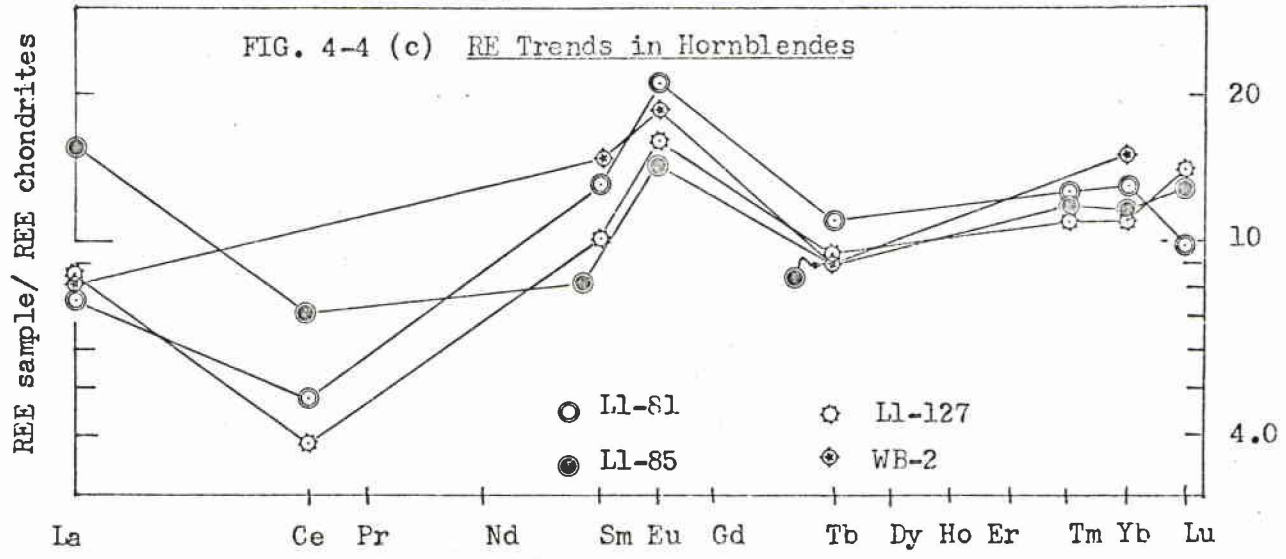

FIG. 4-4 (d) RE Trends in Garnets

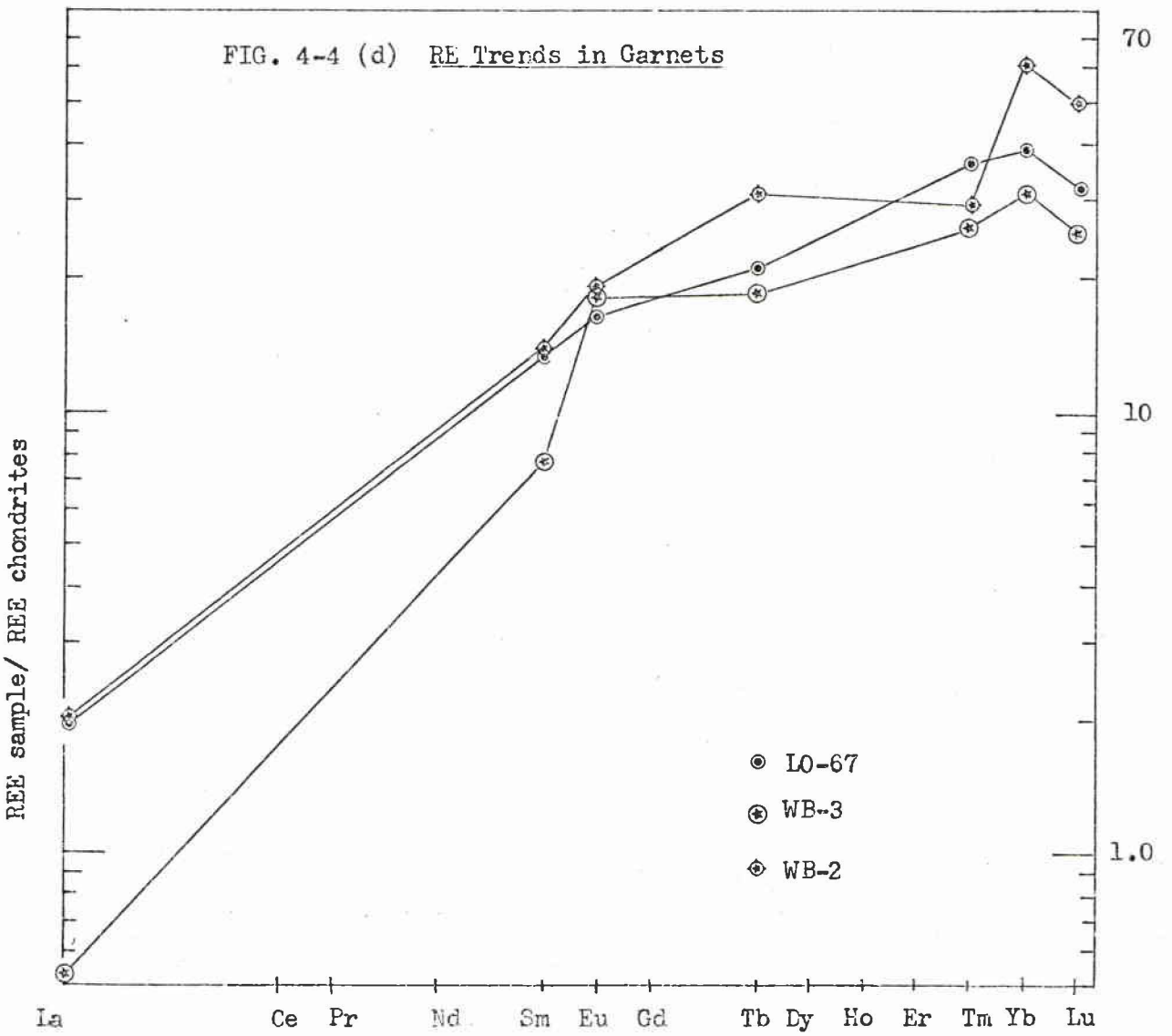

decreases rapidly from La to about Tb, and then remains constant or increases slightly from Tb to Lu (data is scarce for the heavy REE). All plagioclase show anomalously high fractionation of Eu relative to the chondrites. This trend is common to all feldspars (Schnetzler and Philpotts, 1970; Towell et al, 1965), although the enrichment in the light REE is not always as great as shown for the Whitestone plagioclase.

The crystal-chemistry of plagioclase is very complex and no information was found concerning labradorite, the plagioclase in this anorthosite. Inferences will have to be made from consideration of the plagioclase end-members - albite and anorthite. Kempster et al (1962) give bond lengths for Ca-O averaging 2.52 Å (Ca is in 6,7-fold coordination) in anorthite. Ferguson et al (1958) present bond lengths for Na-O averaging > 2.64 Å (Na is in 6-fold coordination) for low albite. Assuming the average bond length, Ca-O, Na-O, is intermediate in labradorite at ≥ 2.58 Å, using Whittaker and Muntus' ionic radius of oxygen (6-fold coordination) of 1.32 Å, then the Ca, Na site has a radius of ≥ 1.26 A. The largest RE^{3+} ion has a radius of 1.13 Å (La^{3+} in 6-fold coordination), however, the Eu^{2+} ion has a radius of 1.25 Å in 6-fold coordination. Thus, it would seem that all the RE^{3+} ions will fit into the Ca^{2+}-Na^{+} site in the plagioclase structure, but the larger ions, and particularly Eu^{2+}, are favoured. This follows from Goldschmidt's rules for ionic substitution into a crystal site, ions most favoured are those having the closest correspondence in ionic radius to that of the site. The introduction of much smaller RE^{3+} ions into large sites is probably more complicated and less energetically favoured.

To confirm the high ratio of Eu^{2+}/Eu^{3+} in plagioclase expected from crystal-chemical considerations, Philpotts' (1970) method of Eu^{2+}/Eu^{3+} calculation must be introduced. Assumption of the equivalence of Eu^{2+} and Sr^{2+}

interphase partitions permits Philpotts to calculate the Eu^{2+} and Eu^{3+} concentrations in each of two equilibrated phases of known Sr and RE concentrations. The equivalence of Eu^{2+} and Sr^{2+} partition coefficients is expected because of their identical ionic radii (1.33 A in 8-fold coordination, according to Whittaker and Muntus, 1970). Also, when this calculation is applied to multiphase rock samples, internal consistency is good. However, even Philpotts suggests that independent analytical and experimental checks should be made before this calculation is accepted as valid. Using the RE and Sr data for samples L0-67 and L1-127 shown in Table 3-5, and Philpotts' relationship:

$$Eu^{3+}_{plag.} = \frac{Eu_{pyx} - \left(\frac{Sr_{pyx}}{Sr_{plag}}\right) \cdot Eu_{plag}}{\frac{Eu^{3+}_{pyx*}}{Eu^{3+}_{plag*}} - \frac{Sr_{pyx}}{Sr_{plag}}}$$

(* where values are obtained by extrapolation from Sm to Gd or Tb)
the Eu^{2+}/Eu^{3+} ratio was found to be 2.4 and 2.0 respectively. This tentatively supports the crystal-chemically suggested conclusion that the anomalous Eu value for Whitestone plagioclase is due to favoured incorporation of the larger Eu^{2+} ion in the plagioclase structure.

4-3-iii. Clinopyroxene-RE Crystal-Chemistry

The chondrite-normalized fractionation trends for clinopyroxenes are almost identical (see Figure 4-4b). Considering the possibly low results for Ce, the fractionation of La, Ce and Tb through Lu relative to the chondrites is rather constant (pyroxene REE are 8-15 times chondrite abundances). A major feature of the trends is the higher fractionation in the Sm-Eu area, and the strong positive fractionation of Eu compared with its neighbours.

Such positive Eu anomalies are usually found only in feldspars (Schnetzler and Philpotts, 1970; Towell et al, 1965), and are interpreted as favoured Eu^{2+} incorporated into the feldspar structure.

In these clinopyroxenes there is some indication that Eu^{3+}, not Eu^{2+} is being incorporated. Consider the most probable cation sites of RE ions in the clinopyroxene structure. Clarke et al (1969) give values of the average oxygen-M_1 and oxygen-M_2 bond lengths in both a diopside and augite as tabulated below:

	diopside	augite
M_1 site occupancy (mole fraction)	mainly Mg	0.72 Mg, 0.18 Al 0.10 Fe
average O-M_1 bond length	2.08 Å	2.05 Å
M_2 site occupancy (mole fraction)	mainly Ca	0.62 Ca, 0.19 Mg, 0.11 Fe, 0.09 Na
average O-M_2 bond length	2.50 Å	2.48 Å

Taking the ionic radius of oxygen of Whittaker and Muntus (1969) as 1.34 Å in 8-fold coordination and 1.32 Å in 6-fold coordination, the approximate radius of the M_1 cation is 0.76 A and the M_2 cation is 1.15 Å. The M_1 site would seem to be too small for the RE^{3+} ions, while all sites are too small for the large Eu^{2+} ion. Also the M_2 cation radius corresponds to the Eu^{3+} radius, suggesting that the maximum in the pyroxene fractionation trend might indicate favoured substitution in the M_2 site by Eu^{3+} and its neighbours. This assumes that the most favoured ion is the one with radius closest to that expected in the site. Masuda and Kushiro (1970) used the same sort of argument in accounting for the RE distribution in the system: diopside-enstatite -H_2O at 20 kb. They found the maximum of the RE partition

coefficients between diopside and glass at Dy^{3+} and used Ahrens' ionic radii (6-fold coordination) to show the similarity of Dy^{3+} and Ca^{2+} radii. They concluded that REE ions occupy the M_2 site in diopside. A similar conclusion is suggested in these clinopyroxenes because of the correspondence of M_2 site radius and Sm^{3+}, Eu^{3+}, Gd^{3+} radii, and the maximum in this area of the RE fractionation trend for clinopyroxene.

The unexpected positive Eu anomaly does not necessarily reflect incorporation of Eu^{2+} into the anorthosite clinopyroxenes. Using the available Sr data for sample LO-67 and following the calculations of Philpotts outlined earlier, the ratio of Eu^{2+}/Eu^{3+} in that clinopyroxene was found to be very low - 0.009. This calculation and its assumptions have not been thoroughly tested, so the low Eu^{2+} abundance is only tentatively implied. However, there seems every indication of Eu^{3+}, not Eu^{2+}, incorporation into the Whitestone clinopyroxene structure. The effects of liquid RE concentrations and more complicated crystal-chemical effects are not dealt with here.

4-3-iv. Hornblende-RE Crystal-Chemistry

The consistency of the chondrite-normalized hornblende RE patterns and the marked similarity of hornblende-clinopyroxenes pair patterns is shown in Figures 4-4c and 3-3. One would expect, then, that the hornblende and clinopyroxenes would have similar sites available for the RE ions. Papike et al (1969) indeed give M_1, M_2, and M_3 bond lengths for a tremolite and a hornblende virtually equal to M_1 sites in a diopside and an augite quoted earlier (page 52). A similar correspondence between amphibole M_4 sites and pyroxene M_1 sites is found. Thus, it seems the chondrite-normalized RE trend in the hornblende reflects a similar crystal-chemical situation

found in the clinopyroxenes of the Whitestone anorthosite.

This is compatible with the conclusion of Mason that the hornblende is secondary after the pyroxenes and probably formed mainly from them, but does not rule out a primary origin for the hornblende. Mason cites petrographic and major element compositional evidence that plagioclase and an Fe rich fluid phase were involved in the breakdown of pyroxene to hornblende. This is not reflected in the RE fractionation trends as no plagioclase type trend seems to have been superimposed on the pyroxene-like hornblende trend. However, this may be due to the minor volume of Σ^{RE}cations taken from both the plagioclase and fluid phases compared to the volume of cations originally in the clinopyroxene. Thus, the hornblende, chondrite-normalized RE patterns probably reflect the substitution of RE ions in the large M_4, 8-fold coordinated site, and reflect the major contribution of REE by the pyroxene to the hornblende structure.

4-3-v. Garnet-RE Crystal-Chemistry

A stronger enrichment in heavy REE than of light REE is a characteristic of all garnet analyses in this work, (see Figure 4-4d) and elsewhere (Schnetzler and Philpotts, 1970 - dacite; Haskin et al, 1966 - eclogite; Vlasov, 1966 - gabbro). This trend is radically different than the plagioclase, pyroxene and hornblende ones.

Geller, based on studies of mixed RE-iron garnet systems (1967), states: "all trivalent RE ions are known to enter c (8-fold coordinated) sites in the garnets. The small trivalent ions of Lu, Yb, Tm, Er, Ho, and Dy also enter a (6-fold coordinated) sites". The preference of Y-Fe garnets for small RE^{3+} ions is indicated by a replacement of only about 1% of the Y^{3+} by Ce^{3+} in Y-Fe garnet when a theoretical replacement of 30% should be possible. In a grossularite from Mexico, Abrahams and Geller (1958) found the

average c site bond distance (c-oxygen) to be 2.41 Å. Using the radius of oxygen of 1.34 Å (8-fold coordination) the c site radius is about 1.07 Å which corresponds to the 8-fold coordination Tm^{3+} radius. The smaller RE^{3+} ions seem to be preferred in the 8-fold as well as the 6-fold coordination sites in garnet, although the complexity of garnet structures makes such a conclusion qualitative at best. This would, however, satisfy the favoured incorporation of heavy REE indicated by the garnet RE fractionation relative to chondrites.

Petrographic evidence suggests a complicated origin for the garnets in the Whitestone anorthosite. Mason (page 184) suggests a late stage formation of garnet involving oxides, pyroxene, hornblende and plagioclase, with the spatial relationships complicated by the development of foliation.

What is the source of the heavy REE found in the Whitestone garnets? If plagioclase, hornblende and pyroxene phases are involved in garnet formation, a depletion (of heavy REE) in at least one phase from garnet-bearing samples is expected. No major differences are observed in pyroxene, hornblende, or plagioclase RE fractionation trends between garnet-bearing and garnet-free samples. Possibly the source of the REE, particularly the heavy REE Sm through Lu, is the late stage, residual fluid phase and/or Fe-Ti oxides. Since no sample of the fluid phase is available and no Fe-Ti oxides were analyzed, their contribution of REE to the garnet can only be inferred. Smith (1970) in a study of coexisting sphene, perovskite, and Fe-Ti oxides for nephelinite lavas found an average of 1.6% and 5.6% REE in sphene and perovskite. Thus the residual Fe-Ti rich fluid phase which probably contains significant Ca as well, is inferred to contain significant concentrations of REE. Occasional blebs of sphene enclosed in garnet emphasizes the

possibility of the Fe-Ti rich fluid phases's participation in garnet development.

4-4. Anorthosite RE Patterns - The Influence of Mineralogy

In true anorthosites the effect of minor phases on the plagioclase-dominated RE fractionation pattern is probably insignificant. But, when the content of minor phases such as olivine and clinopyroxene increases, as in gabbroic anorthosites, the effect is seen. The anorthosite and plagioclase REE enrichment trends are no longer the same. To gauge the effect of these minerals on the plagioclase RE pattern, typical RE fractionation trends for olivine, clinopyroxene and plagioclase are shown in Figure 4-5.

The low RE content of olivine would reduce any modification it would impose on the plagioclase-dominated anorthosite RE trend. The olivine RE trend shows a more constant RE enrichment than does the plagioclase RE trend but the presence of olivine in anorthosite should have only a slight effect on the plagioclase-domination pattern due to the low concentrations of REE in olivine. However, the anorthosite will have a reduced, but still positive, Eu anomaly in its fractionation pattern compared to the plagioclase pattern. At least part of the reason for the rather constant RE enrichment pattern of lunar anorthosites (Figure 4-2) may be attributed to the presence of olivine.

Clinopyroxene should affect the plagioclase-type anorthosite pattern only for REE heavier than Ce, as La and Ce concentrations in clinopyroxene and plagioclase are similar. The anorthosite RE trend should show more enrichment in the heavier REE (Sm-Lu) with clinopyroxene present than does a simple plagioclase-type anorthosite trend. The smaller positive Eu anomaly in the clinopyroxene RE pattern than in the plagioclase RE pattern should

give the clinopyroxene-bearing anorthosite a slightly smaller Eu anomaly than expected by considering the anorthosite equivalent to plagioclase. In the Whitestone anorthosite, which contains clinopyroxene, the only slight decrease in RE enrichment from Sm to Lu (Figure 4-1) reflects the above clinopyroxene effect. The whole rock and plagioclase RE patterns are similar for La and Ce as expected. The Eu anomaly of the anorthosite is slightly smaller than that of the Whitestone plagioclase also as predicted.

Characteristic layered intrusive-type, metasomatic or anatectic type, etc. anorthosite RE trends are not expected to be found. In discussion and comparison of anorthosite RE fractionation patterns, the mineralogy must be considered. Variations in anorthosite RE trends not only reflect environment of formation, but also reflect mineralogical and chemical restrains. In order to speculate on the origin of the Whitestone anorthosite, therefore, mineral RE trends as well as whole rock trends are considered.

4-5. Discussion of Country Rock RE Trends

In an attempt to clarify the anorthosite-country rock relationship, three samples, two from the contact metamorphic aureole and one removed from the aureole were analyzed for RE content. No mineral separates were analyzed and so the chondrite-normalized RE fractionation trends (Figure 4-6) are difficult to discuss. The scarcity of complete RE metamorphic rock data makes comparisons with other areas difficult. Some RE fractionation trends for acidic igneous rocks and metamorphic rocks are shown in Figure 4-7.

Samples S-32 and WB-4, both granitic gneisses, show RE fractionation trends common to acidic igneous rocks and metamorphic gneisses. Sample WB-4, an intrusive granitic sill, is of particular interest. Being intru-

FIG. 4-5 Typical RE Trends in Some Minerals

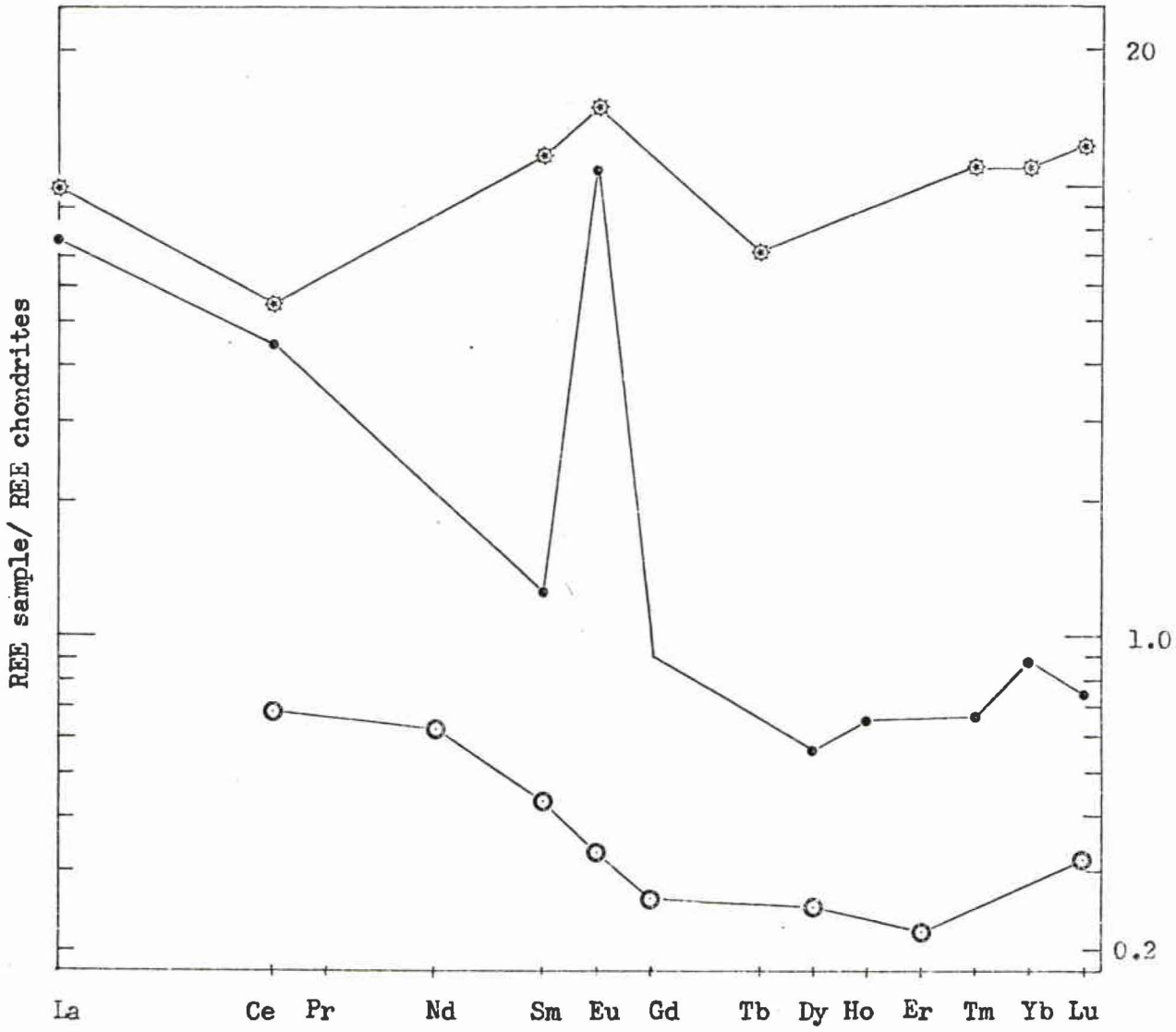

⊙ Olivine, HHP-66-19 Oceanite, Hawaii (Schnetzler and Philpotts, 1970)

⊛ Clinopyroxene, L1-127 (this work)

• Plagioclase, San Marcos Gabbro (Towell et al, 1965a)

sive, it might be comagmatic with the anorthosite. On the basis of these whole rock RE fractionation trends, it is impossible to evaluate the possibility that the granite gneiss, WB-4, crystallized from a Eu-depleted liquid, i.e. that the granite gneiss and Whitestone anorthosite are comagmatic.

The sample closest to the anorthosite (< 100 feet from the contact) Mum-2, an amphibolite, shows a RE fractionation pattern not unlike that of the Cornwall amphibolite (Figures 4-5, 4-7 respectively) Mum-2, however, has a much higher overall RE content. Oxygen isotope studies (R. Mummery, McMaster - personal communication) suggest some exchange between the anorthosite and country rock has occurred and it is interesting to speculate that this exchange could have involved addition of REE to the country rock either from the anorthosite or the late-stage residual fluid phase.

4-6. Origin of the Whitestone Anorthosite

The origin of the Whitestone anorthosite will now be discussed in terms of the RE data and the general theories of anorthosite genesis noted in section 1-3. It must be stressed that this discussion deals only with the Whitestone anorthosite, but a similar treatment of other anorthosite massifs might be successful.

4-6-i. Theories of Type 1 - Anorthosite is a Cumulate Rock

In this category, anorthosites are supposed to represent a cumulate rock developed by fractional crystallization from a magma. The three main parental magma types suggested are dioritic, olivine basaltic (alkali olivine basalt), and alkali basaltic.

The ophitic and possibly poikilitic texture of the Whitestone anorthosite suggests initial crystallization of cumulate plagioclase followed

FIG. 4-6 RE Trends for Country Rock Samples

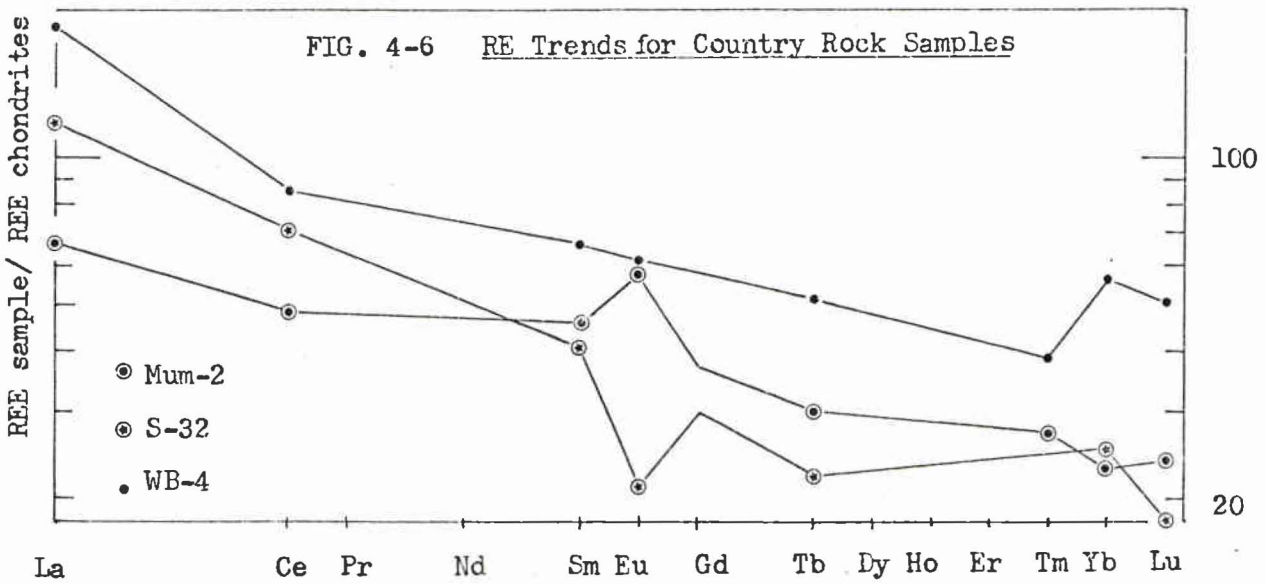

FIG. 4-7 RE Trends for some Metamorphic and Acidic Igneous Rocks

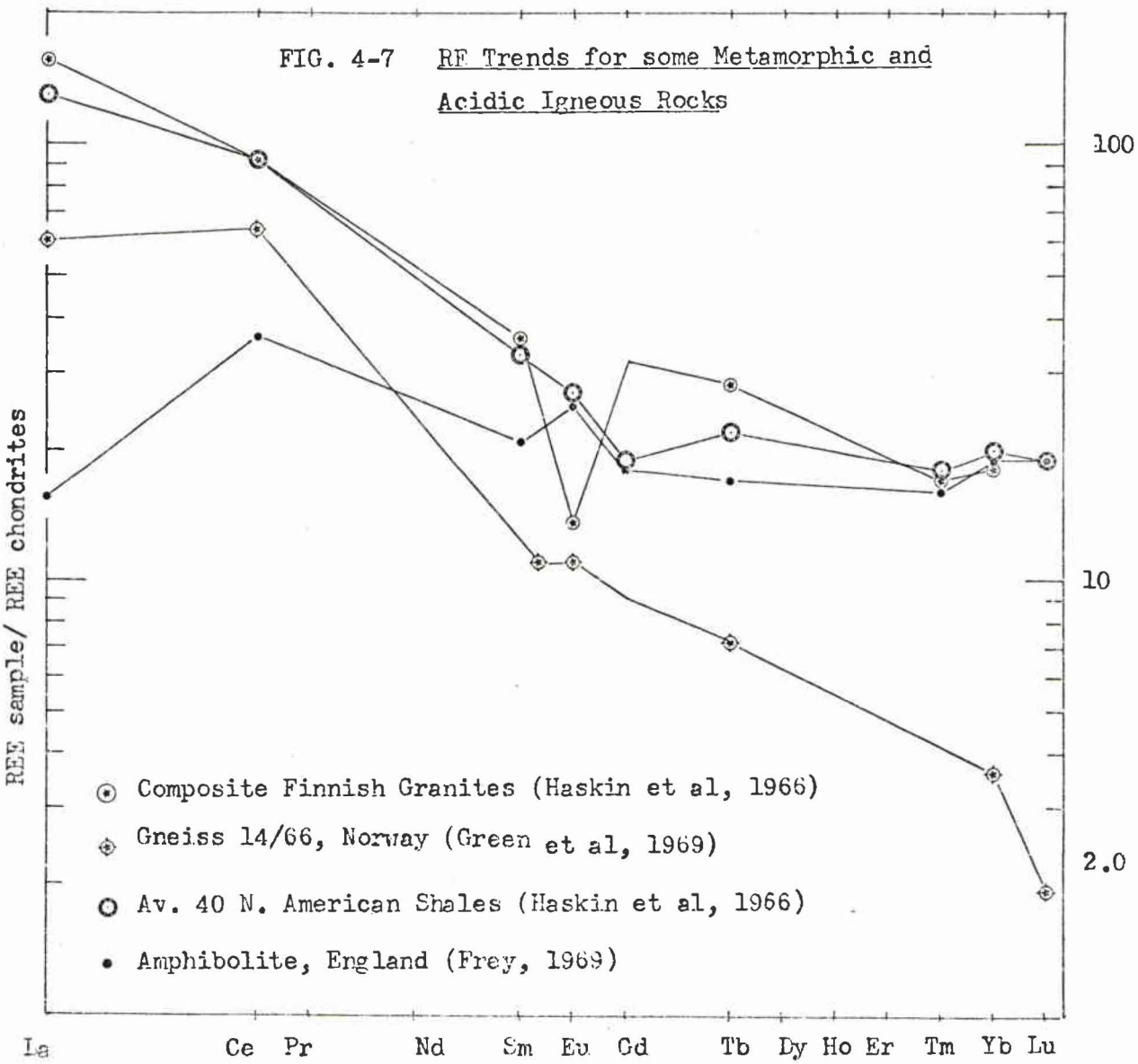

by clinopyroxene plus plagioclase from the intercumulate liquid (Mason, page 238).

One of the most significant features of the REE distribution in this anorthosite is the maximum in the chondrite-normalized REE fractionation trend of clinopyroxene in the Sm-Eu area. In particular, the positive Eu anomaly was unexpected in the clinopyroxene since it crystallized after a Eu concentrating phase-plagioclase. Plagioclase crystallization should deplete the residual liquid in Eu relative to the neighbouring REE and the crystallization of another Eu-enriched (relative to chondrites) phase is unusual. Perhaps the liquid from which the anorthosite crystallized was enriched in Eu relative to the chondrites.

The Calculated Composition of the Mother Liquid

Mass balance calculations are carried out to determine the RE enrichment pattern of the liquid from which the Whitestone anorthosite might have accumulated. The attack follows these lines:

1. Sample L1-127 was chosen as representative of the RE distribution in the Whitestone anorthosite. This sample has the most complete RE mineral analyses and they, along with the whole rock RE analysis, are typical of the anorthosite. L1-127 clinopyroxene, along with plagioclase, is assumed to have crystallized from a residual liquid remaining after plagioclase alone, with a RE content of L1-127 plagioclase, crystallized from the "mother liquid". The excess residual liquid is assumed to be removed.

2. The crystallization of clinopyroxene from the plagioclase-depleted residual is assumed to have pyroxene-liquid REE partition coefficients similar to the clinopyroxene-matrix REE partition coefficients of GSFC-266, rhyodacite (Schnetzler and Philpotts, 1970) shown below:

REE	La	Ce	Sm	Eu	Gd	Tb	Tm	Yb	Lu
Partition coefficient	0.50	0.646	1.81	2.01	1.41	1.18	1.10	1.14	1.28

The clinopyroxene from this *rhyodacite* is rather similar in major element chemistry, particularly Ca/Mg ratio, to the clinopyroxene in the Whitestone anorthosite. The RE partition coefficient trend has a maximum at Sm-Eu, which is expected from the clinopyroxene crystal-chemistry considerations discussed in section 4-3-iii.. The absolute value for each RE partition coefficient in sample GSFC-266 may not be representative of the case considered above.* The absolute value of partition coefficients will depend upon such factors as liquid RE composition, liquid content of other cations, and temperature and will not be constant in different environments. However, it is proposed that the relative values for the RE partition coefficients, or the trend of the RE partition coefficients of sample GSFC-266 are representative of, and constant for, Whitestone anorthosite-type clinopyroxene crystallization considered above.

3. From the relative REE partition coefficients and the RE concentrations in the clinopyroxene, the relative RE concentrations of residual liquid, from which the clinopyroxene crystallized, can be calculated. For each RE:

$$\text{conc. RE}_{\text{liquid}} = \frac{\text{conc. RE}_{\text{clinopyroxene}}}{\text{RE partition coefficient}}$$

* Note: The absolute values of the clinopyroxene-liquid partition coefficients assumed here are not necessarily correct, but their overall trend is considered accurate. The chondrite-normalized RE fractionation trend will be compared with trends from the literature after this calculation. The RE enrichment relative to chondrites is calculated using the assumed partition coefficients, so the absolute RE enrichments are not necessarily correct, but the trend of enrichments is considered accurate.

4. This residual liquid has remained after plagioclase crystallized from the mother liquid. In order to bracket the actual amount of mother liquid that solidified as plagioclase, assume two cases:

1. 10% of the mother liquid solidifies as plagioclase L1-127
2. 80% of the mother liquid solidifies as plagioclase.

The relative RE concentration in the mother liquid can now be calculated for each case using the following equation for each RE:

Case 1: $RE_{\text{mother liquid}} = 0.10\ RE_{\text{L1-127 plag.}} + 0.90\ RE_{\text{residual liquid}}$

Case 2: $RE_{\text{mother liquid}} = 0.80\ RE_{\text{L1-127 plag.}} + 0.20\ RE_{\text{residual liquid}}$

Table 4-3, page 64, summarizes the actual calculation.

The chondrite-normalized RE patterns of the hypothetical "mother liquid" from which the Whitestone anorthosite could have crystallized is shown in Figure 4-8. As the degree of plagioclase crystallization preceeding clinopyroxene increases, the size of the positive Eu anomaly required in the mother liquid increases, and the enrichment in light REE relative to heavy REE increases.

The theories of type 1 postulate diorite or alkali basalt (olivine basalt included) as the parental liquid. Consider first the diorite magma. The best estimate of the RE pattern of dioritic magmas comes from Haskin's et al (1966) composite of samples with $50\% < SiO_2 < 60\%$ (mainly diorites and andesites). This diorite-andesite composite RE pattern is also shown in Figure 4-8. It is quite similar to the trend of the calculated mother liquid (80% plagioclase crystallization) with a steeply decreasing enrichment from La to Sm and a flatter trend from Sm to Yb-Lu. Interestingly, the dioritic magma RE trend shows a positive Eu anomaly. It would seem,

Table 4-3: Calculation of Relative RE Concentration in the Mother Liquid

REE	Pyroxene L1-127 (ppm)	Relative Partition Coefficients GSFC-266	Residual Liquid (relative conc.)	Plagioclase L1-127 (ppm)	Case 1: Mother Liquid relative conc.	Case 1: Mother Liquid Normalized to Chondrites	Case 2: Mother liquid relative conc.	Case 2: Mother Liquid chondrite-normalized
La	2.97	(0.50)	5.9	2.79	5.6	19	3.4	11
Ce	4.60	0.646	7.1	4.05	6.8	8.1	4.6	5.5
Sm	2.47	1.81	1.4	0.20	1.46	7.0	0.44	2.1
Eu	1.10	2.01	0.55	0.25	0.53	7.2	0.31	4.2
Gd	(2.9)	1.41	2.1	(0.20)	1.9	5.9	0.58	1.8
Tb	0.41	(1.18)	0.35	0.03	0.32	5.5	0.094	1.6
Tm	0.28	(1.10)	0.25	0.019	0.23	7.0	0.065	2.0
Yb	1.85	1.14	1.6	0.10	1.4	8.2	0.90	2.4
Lu	0.38	1.28	0.30	0.01	0.27	8.7	0.068	2.2

Note: bracketed values were obtained by extrapolation assuming non-anomalous behavior of the RE of interest.

FIG. 4-8 RE Trends - Possible Parental Magmas

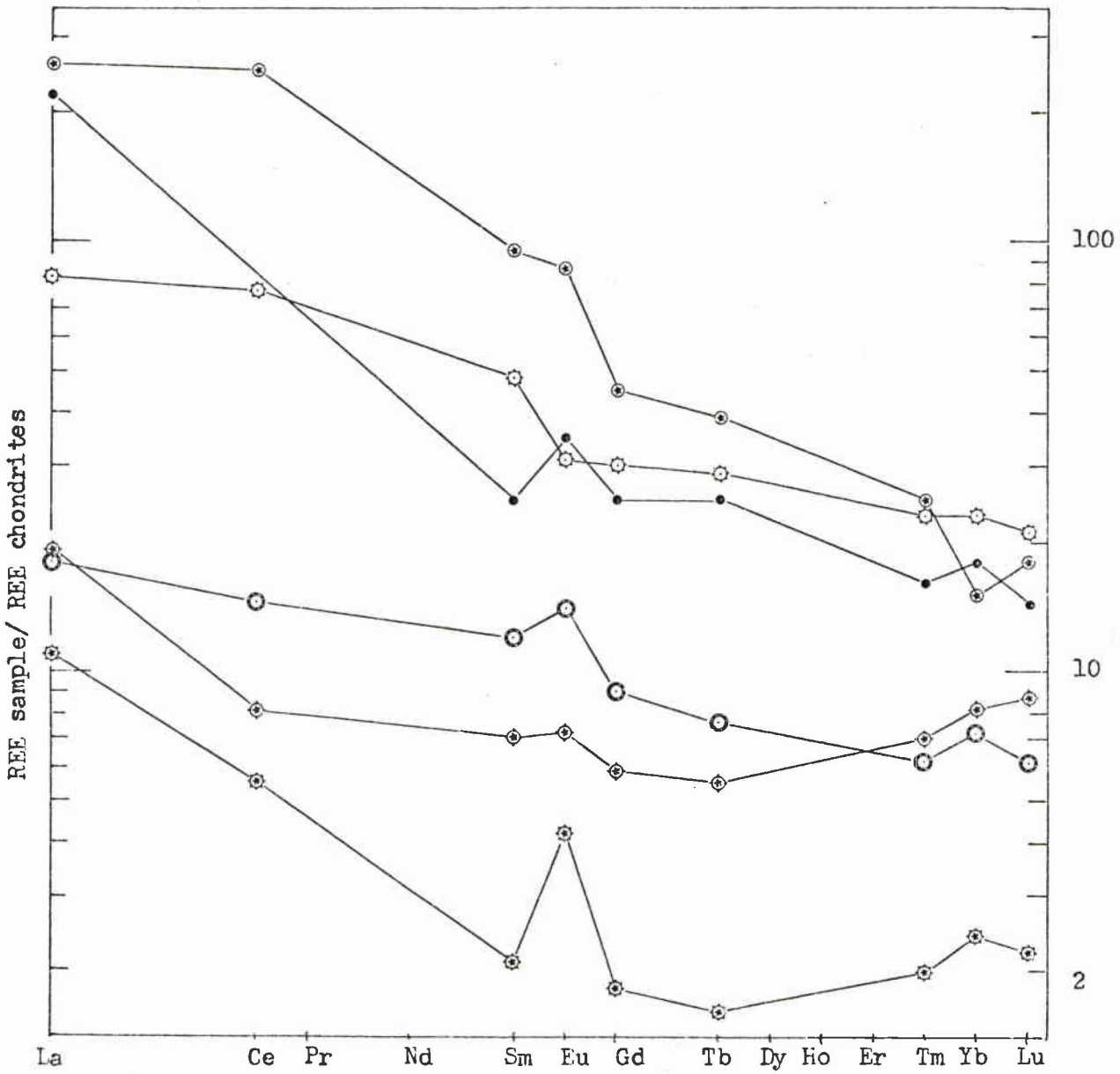

then, that fractional crystallization of a dioritic magma, with about 50% (?) of the magma solidifying as plagioclase, satisfies the RE requirements for the origin of the anorthosite.

What about fractional crystallization of alkali or for that matter, tholeiite basaltic magmas as the origin of this anorthosite? As a representative of alkali basaltic magma the Colorado Plateau basalt, and as a representative of tholeiite basaltic magma, the Columbia Plateau basalt, are included in Figure 4-7. Neither RE trend seems to resemble the trends of the calculated mother liquids.

If these typical alkali and tholeiite basaltic magmas had undergone fractional crystallization prior to massive plagioclase solidification then the RE pattern of the original liquid might be altered by this prior crystallization to the extent of making it similar to that of the required mother liquid. That is, a residual magma- originally alkalic or tholeiitic basalt - might have a RE fractionation pattern similar to the calculated mother liquid of the Whitestone anorthosite. What would be the effect on a basaltic magma of fractional crystallization of peridotite, dunite, or pyroxenite from it? Crystallization of ultrabasic material would have little effect on the relative RE content and the chondrite-normalized RE trend of these basalts because of the much smaller concentration of REE in ultrabasic rocks. For peridotites, pyroxenites and dunites analyzed by Frey et al (1971) and Frey (1969) the Σ REE < 4 ppm, while the composite basalt (Frey et al, 1969) has Σ REE = 189, almost 50 times that of the ultrabasics. Calculations of the effect on a composite basaltic magma of 80% solidification of ultrabasics shows a change in Eu/Sm ratio of $<1\%$! Thus crystallization of ultrabasic rock will not alter the RE

trend of alkalic and tholeiitic basalts significantly.

At this point, a most interesting observation is presented. High Al tholeiitic magma, as possibly represented by the Skaegaard chill zone gabbro, has a strong, positive Eu anomaly and an overall chondrite-normalized RE trend not unlike that for the calculated mother liquid of the Whitestone anorthosite (see Figure 4-8). The major difference between the Skaegaard and calculated mother liquid is the greater enrichment in light REE (relative to heavy REE) of the calculated mother liquid. The major differences between the Skaergaard gabbro and the tholeiitic basalts seem to be environment of crystallization and the high Al content of the Skaergaard tholeiitic magma. No explanation of the positive Eu anomaly observed in the Skaergaard, or for that matter in the Bushveld and Stillwater tholeiitic chill zones (all analyzed by Frey et al, 1969) in light of the usually negative Eu anomaly in tholeiitic basalt magma, the Columbia and Deccan Plateaus (Frey et al, 1969) for example has been suggested. This seems to add high Al tholeiitic magma as another possible parental magma for the Whitestone anorthosite.

It seems then, that simple fractional crystallization from either dioritic or Skaergaard-type, high-Al tholeiitic magma meets the RE requirements as possible origins of the Whitestone anorthosite. Petrologic considerations and field relationships must be taken into account.

Mason rejected an early accumulation of plagioclase from a dioritic magma because the metasomatic contact aureole surrounding the anorthosite implies that no further fractionation took place and that the anorthosite represents the final crystallization product. The possibility exists that the anorthosite was formed elsewhere, remobilized by partial melting

and injected into its present surroundings. The cataclastic texture, and the marginal foliation of the anorthosite are consistent with its injection as a mush of plagioclase crystals in a liquid formed by partial melting of an anorthosite. The occasional banding observed (Mason, plate 2-4, page 36, for example) in the anorthosite also suggests the anorthosite is a cumulate rock. Experimental work by Green (1968) suggests that the product at 50% crystallization of a quartz diorite magma (9-13 kb pressure) is gabbroic anorthosite. There is then both RE and experimental evidence to suggest a dioritic magma as parental material for the Whitestone anorthosite. Remobilization and intrusion of the anorthosite into the present setting may also be required to account for the field relationships.

Similarly, the crystallization of an anorthosite body from a high Al, tholeiitic magma elsewhere, partial melting and in ection into its present surroundings satisfies the field relationships. However, Mason presents persuasive evidence that the high alumina content of the anorthosite clinopyroxene excludes even the high Al tholeiitic magma as parental material. Therefore, the fractional crystallization of an anorthosite from this magma type seems incompatible with the petrologic evidence.

4-6-ii. Theories of Type 2 - Anorthosite Crystallized from a Contaminated Magma

These theories assume basaltic (Michot, P., Kranck) or dioritic (Philpotts) magmas are contaminated by crustal rock. Michot and Kranck postulate almost complete crystallization of this contaminated magma, while Philpotts postulates crystal accumulation for the origin of anorthosites.

What is the effect on a basaltic RE fractionation trend of assimilation of vast quantities of pelitic sediments (à la Michot)? The best estimate of the RE content of sediments or crustal material is probably the average of 40 North American shales (Haskin et al, 1966). A good estimate of basaltic RE content is the "composite" basalt of Frey et al (1969). The REE content of the "plagioclase" magma (Michot, Kranck) which crystallized as anorthosite can be estimated as a combination of equal parts of basalt and sediment. The REE trend for this contaminated magma is compared to the Whitestone anorthosite "composite" in Figure 4-9. The trends are very different, and so assimilation of sediments by a basaltic magma and then crystallization of this magma as an anorthosite is not compatible with REE trends in the Whitestone anorthosite. A smaller degree of sediment contamination yields just as poor an approximation of the Whitestone composite RE trend.

Philpotts (1966) derives anorthosite from fractional crystallization of a granodiorite magma formed by assimilation of crustal material by a dioritic magma. Using Haskin's et al (1966) composite of 85, mainly dacite-andesite samples, ($50\% < SiO_2 < 60\%$) RE concentrations as representative of the diorite magma and those of the average of 40 North American shales as representative of the crustal material, the RE trend of the granodiorite magma (assuming a 1:1 ratio of diorite to sediment) is calculated and shown in Figure 4-9. This RE trend approximates the first case of calculated mother liquid of the Whitestone anorthosite, except for a greater enrichment in light REE relative to heavy REE in the granodiorite. Assuming less sediment contamination of the diorite magma does not decrease the similarity of the contaminated magma to the anorthosite

mother liquid. In section 4-6-i, the similarity of the diorite and mother liquid was noted. It seems that both contaminated diorite and diorite magmas can represent the liquid from which the Whitestone anorthosite crystallized by fractional crystallization.

As discussed in the preceeding section, the origin of the Whitestone as a remobilized cumulate rock originally formed by fractional crystallization from a dioritic magma does not contradict the field observations or the RE considerations. This would apply for a contaminated dioritic magma as well.

4-6-iii. Theories of Type 3 - Existence of a Gabbroic Anorthosite Magma

The existence of a gabbroic anorthosite magma is postulated by Buddington (1939, 1961) and Mason. Buddington favours partial fusion of basaltic or mantle material as a source of this magma. This is somewhat analogous to the fractional crystallization of a basaltic magma discussed in section 4-6-i. It was found that the RE trend of liquid remaining after ultramafic crystallization was significantly different from the RE trend of the basalt. Partial fusion of basaltic mantle material, if the residual is ultramafic rock, does not seem to be the source of magma having RE trends similar to the Whitestone anorthosite RE trend. Rather, a basaltic RE trend will persist in the liquid. However, the unusual RE trends seen in the chill zone gabbros from layered intrusives (section 4-6-i), would not require much alteration before they would resemble the Whitestone anorthosite. Figure 4-10 indicates the RE trend developed in the liquid when the Skaergaard chill zone gabbro (≡ basaltic magma) partially melts and 50% by volume remains behind as peridotite (Stillwater peridotite, Frey et al, 1970). The trends of this liquid

FIG. 4-9 RE Trends - Contaminated Magmas

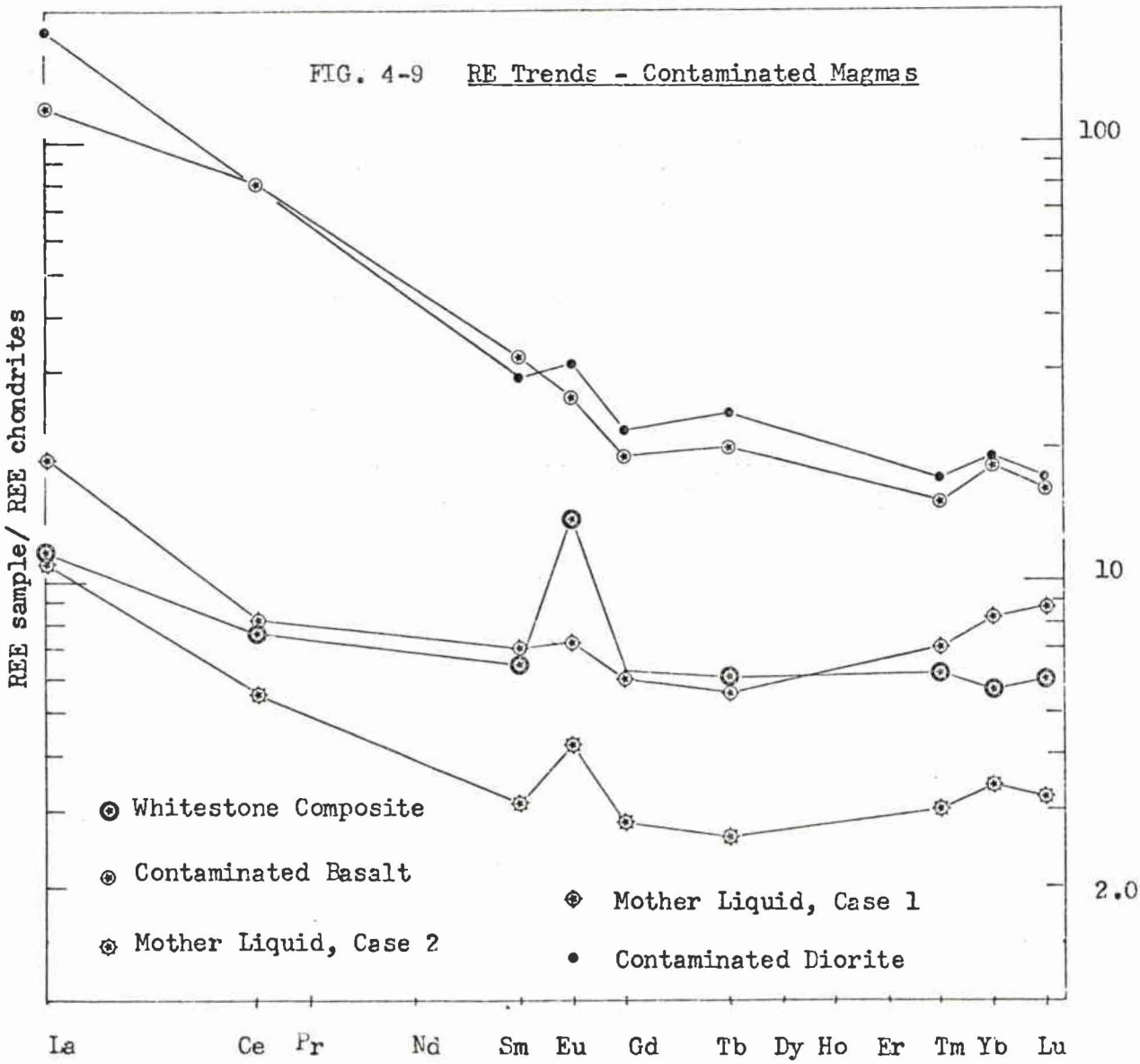

FIG. 4-10 RF Trends - Partial Melting Magma

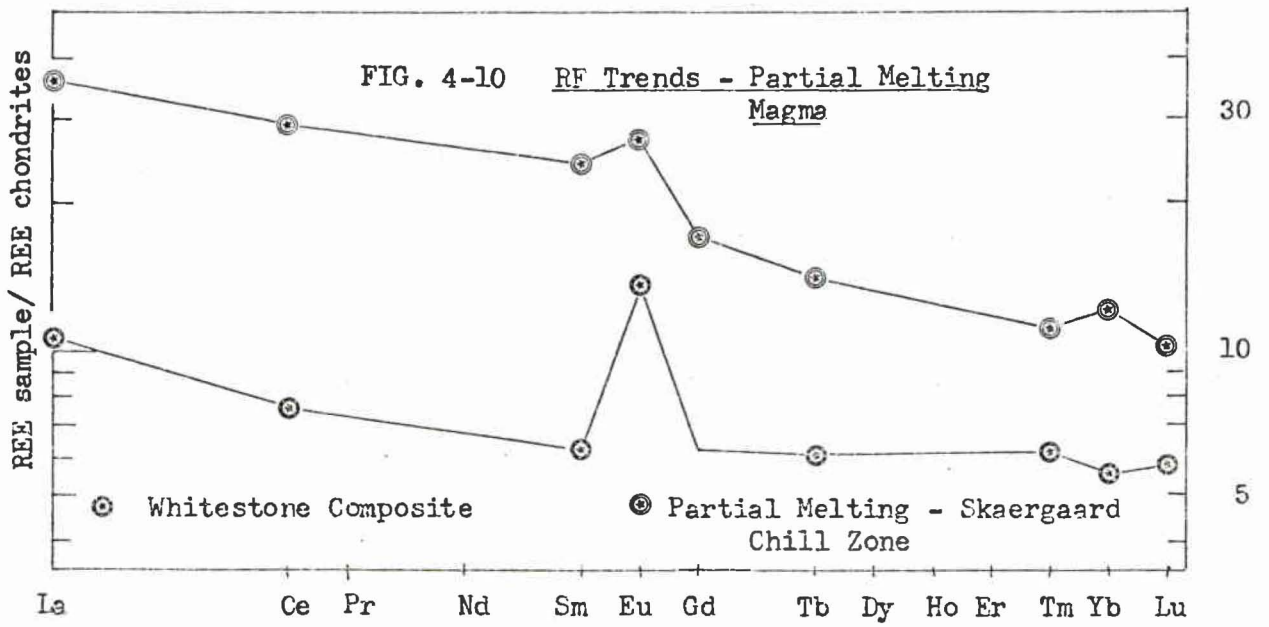

and the Whitestone anorthosite are quite similar with the major differences being the larger Eu anomaly and the flatter heavy RE trend of the anorthosite. Even greater similarity might be achieved if less melting of the basaltic material yielded a more "plagioclase-rich" liquid and a residual of other than ultramafic rock, but this is speculative.

Thus the partial melting of basalt with a residual of ultramafic rock cannot account for the RE trend of the Whitestone anorthosite. The partial melting of unusual (?) basaltic material, represented in chill zones of differentiated complexes, produces a more anorthositic RE trend in the liquid but the petrologic evidence cited in section 4-6-i rejects even high Al tholeiitic magma as parental material for the Whitestone anorthosite.

Mason suggests two other possible sources of a gabbroic anorthosite magma. The first, "fractionating from a basic [= basaltic] magma a mixture of diopsidic clinopyroxene and enstatitic orthopyroxene ... probably with minor basic plagioclase", (Mason, page 236), is considered next. Schnetzler and Philpotts (1970) show phenocryst-matrix partition coefficients for diopside and orthopyroxenes from a mafic phonolite, and andesitic basalts, which have virtually no Eu anomaly. This would indicate that fractionating these minerals from a basaltic magma would not produce a larger positive Eu anomaly in the liquid. This lack of negative Eu anomaly in diopsidic clinopyroxenes and orthopyroxenes is the same fact that seems to make partial fusion of basaltic material with ultramafic residual a poor model for origin of the Whitestone RE trends.

Mason also suggests partial fusion of an amphibolite could theoretically yield a plagioclase-rich liquid (after Yoder and Tilley, 1962, p. 461). Since no hornblendites, the probable residual of this process, have been

analyzed for REE, the RE trend of such a liquid is difficult to establish. An anorthositic RE trend would be expected in any plagioclase-rich (> 80%) material, but lack of RE data on hornblendites and amphibolites makes further speculation difficult.

The origin of a gabbroic anorthosite RE fractionation trend from partial fusion of basaltic material with a residual of ultramafic rock seems unlikely. Partial melting of an amphibolite probably could produce a Eu-enriched RE trend, but lack of data makes further speculation impossible. The existence of a gabbroic anorthosite magma was postulated by Mason after a consideration of field relationships and petrology of the Whitestone anorthosite. The partial melting of an amphibolite to form such a magma is in line with the bulk of evidence and probably would not contradict RE findings.

4-6-iv. Theories of Type 4 - Metasomatism and Anatexis

The anatectic melting of a leuconorite or a noritic anorthosite with the mobilization of most of the mafics and some of the plagioclase leaving behind a residuum of plagioclase is suggested by Michot (1961) as the process forming some Norwegian anorthosites. This case involves almost a secondary origin for gabbroic anorthosites since a noritic anorthosite is assumed to have already existed. Discussion of such a process in terms of REE seems redundant, and such a process, as it applies to the Whitestone anorthosite, is best discussed in terms of textural and petrologic information.

The intrusive nature of the Whitestone anorthosite argues against a metasomatic (para-anatectic) origin for it. However, a remobilized "para-anatectic" anorthosite is possible. The plagioclase morphologies of the Whitestone anorthosite resemble those described by Michot (1961)

in the Haland-Helleren massif. These plagioclase textures of a "para-anatectic" anorthosite would probably be obscured by the recrystallization following remobilization. Therefore, primary para-anatectic textures are not expected in the Whitestone anorthosite if it was remobilized. Mason attributes the plagioclase morphologies to recrystallization in the Whitestone anorthosite - a more probable explanation.

4-6-v. Theories of Type 5 - Disruption of Layered Intrusives

These theories argue for the remobilization of anorthosite and gabbroic anorthosite and destruction of the spatial relationships that make these bands easily recognized as members of a layered series. Again, RE information would be redundant, since metamorphosed and disrupted anorthosite bands would simply retain the original RE trends.

There is no clear evidence of a layered intrusive origin for this anorthosite. No ultrabasic or basic rocks are found in outcrop or suggested by aeromagnetic work. Parallel orientation of plagioclase laths is not common and cryptic layering is not suggested. The remobilization might have obscured some of these layered anorthosite characteristics. Some igneous banding is suggested and occasional block structures, possibly representing disrupted layering are found, but these reflect only a cumulate origin and not a layered-intrusive origin. Because there is no clear evidence of a layered-anorthosite origin for the Whitestone anorthosite, and because RE investigations are not expected to be helpful in defining a layered-intrusive origin, this type of origin will not be considered in the case of the Whitestone anorthosite.

CHAPTER 5

CONCLUSIONS AND RECOMMENDATIONS

5-1. Conclusions

1. The analytical method used in this work was both simple and yet complete enough to define the RE trends of the anorthosite and constituent minerals. The analytical data is of sufficient quality to bear the burden of interpretation placed upon it in this work.

2. As Green et al (1969) found, the anorthosite-country rock relationships are not elucidated by whole rock RE information. There is a suggestion, supported by oxygen isotope data, that REE were released to the country rock from the anorthosite or residual fluid phase. No conclusions on the granitic sill west of the anorthosite regarding co-genetic relationships could be drawn.

3. The RE fractionation trends in the major anorthosite minerals are defined and explained on crystal-chemical grounds.

4. A number of possible modes of origin of the Whitestone anorthosite are suggested from RE data which do not contradict field relationships or major petrologic considerations:

i. The anorthosite represents a cumulate rock originally formed by fractional crystallization from a dioritic (possibly contaminated) magma. This rock was partially melted and intruded into its present setting.

ii. The anorthosite represents crystallization of a gabbroic anorthosite magma which originated by partial melting of an amphibolite.

This was not elucidated by RE inforamtion but is not obviously contradictory to expected RE findings.

iii. The anorthosite represents a disrupted layered-intrusive anorthosite. No proof of this origin is offered and this possibility is only added for completeness.

5-2. Recommendations

1. Improvement in the analytical procedure to determine Nd, Gd and one of Dy, Y, Ho or Er could make more detailed geochemical interpretations possible.

2. RE studies of country rock minerals could elucidate the country rock-anorthosite relationships.

3. Experimental investigation of RE partition between mineral phases of anorthosites would also improve RE geochemical interpretations of anorthosite petrogenesis.

4. Continued geochemical, petrological, and experimental investigations hopefully will solve the problem of anorthosite origin (s).

BIBLIOGRAPHY

Abrahams, S.C. and Geller, S., 1958: Refinement of the Structure of Grossularite Garnet; Acta Cryst., v. 11, p. 437-441.

Balashov, Yu. A., 1963: Regularities in the Distribution of Rare Earths in the Earth's Crust; Geochemistry, 1963, p. 107-124.

Balk, R., 1931: Structural Geology of the Adirondack Anorthosites; Min. u. Pet. Mitt. 41, p. 308-434.

Barth, T.F.W., 1936: The Large Pre-Cambrian Intrusive Bodies in S. Norway; 16th Inter. Geol. Cong. Rept., p. 297-309.

Berg, R.B., 1969: Petrology of Anorthosite of the Bitterroot Range, Montana; Origin of Anorthosites and Related Rocks, Mem. 18, N.Y. State Museum and Science Service, p. 387-397.

Berrange, J.P., 1965: Some Critical Differences between Orogenic-Plutonic and Gravity-Stratified Anorthosites; Geol. Rund. 55, p. 617-642.

Bowen, N.L., 1917: The Problem of the Anorthosites; J. of Geology, v. 25, p. 209-243.

Bridgewater, D., 1967: Feldspathic Inclusions in the Gardar Igneous Rocks and their Relevance to the Formation of Major Anorthosites in the Canadian Shield; Can. J. Earth Sci., v. 4, p. 995-1014.

Buddington, A.F., 1939: Adirondack Igneous Rocks and their Metamorphism; G.S.A. Mem. 7.

Buddington, A.F., 1961: The Origin of Anorthosite Re-evaluated; Geol. Surv. India Records 86, p. 421-432.

Clarke, J.R., Appleman, D.E., and Papike, J.J., 1969: Crystal-Chemical Characterization of Clinopyroxenes Based on Eight New Structure Refinements; Mineral. Soc. Amer. Spec. Paper 2, p. 31-50.

Coryell, C.D., Chase, J.W., and Winchester, J.W., 1963: Procedure for Geochemical Interpretation of Terrestrial Rare Earth Abundance Patterns; J. Geophys. Res., v. 68, p. 559-566.

Emslie, R.F., 1965: The Michikamau Anorthositic Intrusion, Labrador; Can. J. Earth Sci., v. 2, p. 385-399.

Ferguson, R.B., Traill, R.J., and Taylor, W.H., 1958: The Crystal Structures of Low-Temperature and High-Temperature Albites; Acta Cryst., v. 11, p. 331-348.

Frey, F.A., 1969: Rare Earth Abundances in a High-Temperature Peridotite Intrusion; Geochim. Cosmochim. Acta, v. 32, p. 1429-1447.

Frey, F.A., Haskin, M.A., Poetz, J.A, and Haskin, L.A., 1969: Rare Earth Abundances in Some Basic Rocks; J. Geophys. Res., v. 73, p. 6085-6098.

Frey, F.A., Haskin, M.A., and Haskin, M.A., 1971: Rare-Earth Abundances in Some Ultramafic Rocks; J. Geophys. Res., v. 76, p. 2057-2070.

Fritze, K. and Robertson, R., 1969: Precision in the Neutron Activation Analysis for Gold in Standard Rocks G-1 and W-1; Modern Trends in Activation Analysis, Nat. Bur. Stand. (U.S.) Spec. Publ. 312, v.2, p. 1979-2183.

Geller, S., 1967: Crystal-chemistry of the Garnets; Zeitschrift für Kristallographie; v. 125, p. 1-47.

Goldschmidt, V.M. and Thomassen, L., 1924: Videnskaps. Skrift I: Mat-naturv. KL., No. 5.

Goldschmitt, V.M., 1954: Geochemistry, Oxford University Press.

Gordon, G.E., Randle, K., Goles, G.G., Corlis, J.B., Beeson, M.H., and Oxley, S.S., 1968: Instrumental Activation Analysis of Standard Rocks with High-Resolution γ-ray Detectors; Geochim. Cosmochim. Acta, v. 32, p. 369-396.

Green, T.H., 1969: Experimental Fractional Crystallization of Quartz Diorite and its Application to the Problem of Anorthosite Origin; in Origin of Anorthosite and Related Rocks, Mem. 18, N.Y. State Museum and Science Service, p. 23-29.

Green, T.H., Brunfelt, A.O., Heier, K.S., 1969: Rare Earth Element Distribution in Anorthosites and Associated High Grade Metamorphic Rocks, Lofoten - Vesteraalen, Norway; Earth and Plan. Sci. Letters, v.7, p. 93-98.

The Handbook of Chemistry and Physics, 45th ed.; The Chemical Rubber Co..

Hargraves, R.B., 1962: Petrology of the Allard Lake Anorthosite Suite; G.S.A. Buddington Vol. 55, p. 163-189.

Harrison, J.M., 1944: Anorthosites in S.E. Ontario; B.G.S.A., v. 55, p. 1401-1430.

Haskin, L.A. and Gehl, M.A., 1963: The Rare-Earth Contents of Standard Rocks G-1 and W-1 and their Comparison with other Rare Earth Distribution Patterns; J. Geophys. Res., v. 68, p. 2037-2043.

Haskin, L.A., Frey, F.A., Schmitt, R.A., and Smith, R.H., 1966: Meteoritic, Solar, and Terrestrial Rare-Earth Distributions; Physics and Chem. of the Earth, v. 7, p. 167-321.

Haskin, L.A., Allen, R.O., Helmke, P.A., Paster, T.P., Anderson, M.R., Koretev, R.L., and Zweifel, K.A., 1970: Rare Earths and Other Trace Elements in Apollo 11 Lunar Samples; Proc. of the Apollo 11 Lunar Sci. Conference, v.2, p. 1213-1231.

Hietanen, A., 1963: Anorthosite and Associated Rocks in the Boehls Butte Quadrangle, Idaho; U.S.G.S. Prof. Pap. 344-B.

Higuchi, H., Tomura, K., Onuma, N., and Hamaguchi, H., 1969: Rare Earth Abundances in Several Geochemical Standard Rocks; Geochem. J., v. 3, p. 171-180.

Kant, A., Cali, J.P., Thompson, H.D, 1956: Determination of Impurities in Silicon by Neutron Activation Analysis; Anal. Chem., v. 28, p. 1867-1871.

Kempster, C.J.E, Megaw, H.D., and Radoslovich, E.W., 1962: The Structure of Anorthite $CaAl_2Si_2O_8$ II: Description and Discussion; Acta Cryst., v. 15, p. 1017-1035.

Kranck, E.H., 1961: The Tectonic Position of the Anorthosites of Eastern Canada; Com. Geol. Finlande, Bull. No. 196, p. 299-320.

Lacey, W.C., 1960: Geology of the Dunchurch Area, Ontario; B.G.S.A., v. 71, p. 1713-1718.

Lederer, C.M., Hollander, J.M., and Perlman, I., 1967: Table of Isotopes, 6th ed.; John Wiley and Sons, Inc..

Mason, I.M., 1969: Petrology of the Whitestone Anorthosite; Ph. D. Thesis, McMaster University.

Masuda, A. and Kushiro, I., 1970: Experimental Determination of Partition Coefficients of Ten Rare Earth Elements and Barium between Clinopyroxene and Liquid in the Synthetic Silicate System at 20 kilobar Pressure; Contr. Mineral. and Petrol., v. 26, p. 42-49.

Michelsen, O.B. and Steinnes, E., 1969: Determination of Some Rare Earths in Rocks and Minerals by Neutron Activation and Gamma-Gamma Coincidence Spectrometry; Modern Trends in Activation Analysis, Nat. Bur. Stand. (U.S.) Spec. Publ. 312, v.1, p. 315-319.

Michot, J., 1961: The Anorthosite Complex of Haland-Helleren; Norsk. Geol. Tidsk., v. 41, p. 157-172.

Michot, P., 1955: Anorthosites et Anorthosites; Bull. de l'Acad. Royale de Belg. Classe des Sc., 5e serie, p. 275-294.

_____, 1960: La Geologie de la Catazone: Le Problem des Anorthosites; Inter. Geol. Cong. XXI, Guide Book G.

Mosen, A.W, Schmitt, R.A., and Vasilevskis, J., 1961: A Procedure for the Determination of the Rare Earth Elements Lanthanum through Lutetium, in Chondritic, Achondritic and Iron Meteorites by Neutron-Activation Analysis; Anal . Chim. Acta, v. 10, p. 10-24.

Nagasawa, H., 1970: Rare Earth Concentrations in Zircons and Apatites and their Host Dacites and Granites; Earth and Plan. Sci. Letters, v. 9, p. 359-364.

Papike, J.J., Ross, M., and Clark, J.R., 1969: Crystal-chemical Characterization of Clinoamphiboles based on Five New Structure Refinements; Mineral. Soc. Amer. Spec. Paper 2, p. 117-136.

Philpotts, A.R., 1966: Origin of the Anorthosite-Mangerite Rocks in S. Quebec; J. of Pet., v. 7, p. 1-64.

Philpotts, J.A., Schnetzler, C.C., and Thomas, H.H., 1966: Rare Earth Abundances in an Anorthosite and a Mangerite; Nature, v. 212, p. 805-806.

Philpotts, J.A., 1970: Redox Estimation from a Calculation of Eu^{2+} and Eu^{3+} Concentrations in Natural Phases; Earth and Plan. Sci. Letters, v. 9, p. 257-268.

Philpotts, J.A., and Schnetzler, C.C., 1970: Apollo 11 Lunar Samples: K, Rb, Sr, Ba, and Rare-Earth Concentrations in Some Rocks and Separated Phases; Proc. Apollo 11 Lunar Sci. Conference, v. 2, p. 1471-1486.

Plumb, R.C., and Lewis, J.E., 1955: How to Minimize Errors in Neutron Activation Analysis; Nucleonics, v. 13, p. 42-46.

Rankama, K., and Sahama, Th. G., 1950: Geochemistry, University of Chicago Press.

Rey, P., Wakita, H., and Schmitt, R.A., 1970: Radiochemical Activation Analysis of In, Cd, and the 14 Rare Earth Elements and Y in Rocks; Anal. Chem. Acta, v. 51, p. 163-178.

Roy, J.C. and Hawton, J.J., 1960: Table of Estimated Cross-sections for (n,p), (n, 2n) Reactions in a Fission Neutron Spectrum; Atomic Energy of Can. Ltd., CRC-1003.

Sahama, Th.G. and Vähätalo, V., 1941: Bull. Comm. Geol. Finlande, v. 126, p. 51- .

Schmitt, R.A., Smith, R.H., Lasch, J.E., Mosen, A.W., Olehy, D.A., and Vasilevskis, J., 1963: Abundance of the 14 Rare Earth Elements, Sc, and Y in Meteoritic and Terrestrial Matter; Geochim. Cosmochim. Acta, v. 27, p. 577.

Schmitt, R.A., Smith, R.H., and Olehy, D.A., 1964: Rare-Earth, Yttrium and Scandium Abundances in Meteoritic and Terrestrial Matter - II; Geochim. Cosmochim. Acta, v. 28, p. 67-86.

Schnetzler, C.C., and Philpotts, J.A., 1970: Partition Coefficients of Rare-Earth Elements between Igneous Matrix Material and Rock-forming Mineral Phenocrysts - II; Geochim. Cosmochim. Acta, v. 34, p. 331-340.

Smales, A.A., 1971: The Place of Activation Analysis in Geochemistry and Cosmochemistry; in Activation Analysis in Geochemistry and Cosmochemistry, Brunfelt, A. O. and Steinnes, E., editors, p. 17-24.

Smith, A.L., 1970: Sphene, Perovskite, and Coexisting Fe-Ti Oxide Minerals; Am. Mineral., v. 55, p. 264-269.

Subramaniam, A.P., 1956: Petrology of the Anorthosite-Gabbro Mass at Kadavur, Madras, India; Geol. Mag., p. 287-300.

_____, 1956b: Mineralogy and Petrology of the Sittampundi Complex, Salem District, India; B.G.S.A., v. 67, p. 317-390.

Taylor, S.R., 1960: The Abundance of the Rare Earth Elements in Relation to Their Origin; Geochim. Cosmochim. Acta, v. 19, p. 100-112.

_____, 1965: Geochemical Analysis by Spark Source Mass Spectrography; Geochim. Cosmochim. Acta, v. 29, p. 1243-?161.

Tomura, K., Higuchi, H., Miyaji, N., Onuma, N., and Hamaguchi, H., 1968: Determination of Rare-Earth Elements in Rock Samples by Neutron Activation Analysis with a Lithium-Drifted Germanium Detector after Chemical Group-Separation; Anal. Chem. Acta. v. 41, p. ?17-228.

van Tongeren, W., 1938: Contributions to the Knowledge of the Chemical Composition of the Earth's Crust in the East Indian Archipelago II, On the Occurance of Rarer Elements in the Netherlands East Indies, Amsterdam.

Towell, D.G., Volfovsky, R., and Winchester, J.W., 1965a: Rare Earth Abundances in the Standard Granite G-1 and the Standard Diabase W-1; Geochim Cosmochim. Acta, v. 29, p. 269-572.

Towell, D.G, Winchester, J.W., and Spirn, R.V., 1965: Rare-Earth Distributions in Some Rocks and Associated Minerals of the Batholith of Southern California; J. Geophys. Res., v. 70, p. 3485-3496.

Vlasov, K.A. (Ed.), 1966: Geochemistry of Rare Elements; p. 205-277.

Wakita, H., and Schmitt, R.A., 1970: Lunar Anorthosites: Rare-Earth and other Elemental Abundances; Sci., v. 170, p. 969-974.

Whittaker, E.J.W., and Muntus, R., 1970: Ionic Radii for Usin in Geochemistry; Geochim. Cosmochim. Acta, vo. 34, p. 945-956.

Windley, B., 1967: On the Classification of W. Greenland Anorthosites; Geol. Rund., v. 56, p. 1020-1026.

Winkler, H.G.F. and von Platen, H., 1960: Experimentelle Gesteinsmetamorphose III; Geochim. Cosmochim. Acta, v. 18, p. 294-316.

Yoder, H.S., and Tilley, C.E., 1962: Origin of Basalt Magmas: An Experimental Study of Natural and Synthetic Rock Systems; J. of Pet., v. 3, p. 342-532.

APPENDIX A

A-1. Petrographic Description of Samples

Table A-1: Modes for Samples of the Whitestone Anorthosite

No.	An.	Plag.	Scap.	Pyx.	Hb.	Gt.	Ep.	Opg.	Sph.	Others
WB-3	(68) 50[1]	76	tr	13	4	5	-	3	-	1^{B}, tr^{Q}
WB-2	62	80	tr	14	4	1	-	1	tr	tr^{Q}
L1-81[2]	52	37	20	30	11	tr	-	1	tr	-
L1-85	54	68	13	12	6	-	-	tr	tr	1^{Q}
L1-126[3]	77	60	11	22	7	-	-	tr	-	tr^{B}
L1-127[2]	78	37	20	30	11	-	tr	-	-	1^{Q}, tr^{C}
LO-67[3]	50	77	4	4	1	9	-	4	tr	1^{C}
L2-2[2]	57	85	-	-	4	-	10	-	-	tr^{Q}, tr^{B}
WB1-1	60	84	2	-	9	-	5	tr	-	tr^{B}, tr^{Q}
L1-354[2]	55	58	11	1.5	28	tr	-	tr	-	0.5^{Q}, tr^{B}

Notes:
1. (68) refers to the large (> 1 cm.) plag. phenocrysts
   50 refers to the smaller (< 1 cm.) plag. phenocrysts
2. after I. Mason, Ph. D. Thesis.
3. after I. Mason, Ph. D. Thesis, results confirmed by this author.

An. = anorthite content of plagioclase(%)
Plag. = plagioclase
Scap. = scapolite
Pyx. = pyroxene
Hb. = hornblende
Gt. = garnet
Ep. = epidote
Opg. = opaque oxide
Sph. = sphene
B = biotite
C = carbonate
Q = quartz

WB-3: Green Feldspar Facies

The texture of this specimen is subophitic and possibly was poikilitic before recrystallization. Large, euhedral, recrystallized plagioclase grains (An_{68}, up to 3 cm. long) are present, but most plagioclase has recrystallized to subhedral, smaller grains (An_{50}), suggesting the larger grains represent an early crystallized plagioclase. Clinopyroxene occurs as recrystallized, subhedral grains replacing or surrounding primary clinopyroxene which shows oxides exsolved along traces 45° to cleavage. Clinopyroxene is associated with and often rims anhedral, opaque oxide grains. Uralitisation is evident, as clinopyroxene is often rimmed by dark green, anhedral hornblende which often contains quartz blebs. Garnet occurs as euhedral grains in plagioclase fields or as generally subhedral grains surrounding either:

1. recrystallized plagioclase with oxide, minor pyroxene core
2. recrystallized plagioclase with pyroxene, secondary hornblende $\pm$ oxide cores
3. recrystallized plagioclase only.

WB-2: Green Feldspar Facies

An almost totally recrystallized sample with more granitic texture, WB-2 is mainly a plagioclase (An_{62}) mosaic of subhedral, equidimensional grains. Narrow, yellowish veins intruding and surrounding plagioclase grains probably cause the green feldspars apparent in hand specimen. Occasional scapolite occurs, replacing plagioclase. Occurence of recrystallized and unrecrystallized clinopyroxene is generally as in specimen WB-3, but unrecrystallized clinopyroxene is rare. Occasional orthopyroxene rimming clinopyroxene is observed. Hornblende with or without quartz blebs commonly rims clinopyroxene grains. Garnet occurs as in specimen WB-3.

L1-81: Porphyritic Facies (atypically rich in mafics)

L1-81 shows a slightly subophitic texture of recrystallized plagioclase (An_{52}) partially enclosed by generally recrystallized, subhedral clinopyroxene. The subhedral plagioclase grains contain abundant scapolite which occasionally engulfs several grains, but normally is limited to plagioclase interfaces, fractures, and cleavages. Scapolite is found only with plagioclase. The unrecrystallized, subhedral pyroxene has abundant opaque oxides oriented 45° to cleavage. The margins of these plagioclase grains contain recrystallized, subhedral to anhedral clinopyroxene grains often enclosed in a rim of hornblende.

L1-85: Glomeropoikilitic Facies

An ophitic texture is suggested even though both plagioclase (An_{54}) and clinopyroxene have been completely recrystallized into more equidimensional grains. This is most evident in the "glomerules" (see Mason, pages 32-33). Scapolite occurs mainly at plagioclase interfaces. Hornblende, occasionally containing quartz blebs, rims most clinopyroxene and occasionally rims opaque oxide grains.

L1-126: Glomeropoikilitic Facies

In the glomerule, a poikilitic texture is suggested having now partially recrystallized plagioclase enclosed by areas of now recrystallized clinopyroxene. Where pyroxene is more evenly distributed the texture is subophitic. Plagioclase (An_{77}, anomalously calcic) grains are not equidimensional, but show a cataclastic texture of large unrecrystallized (?) grains in a matrix of smaller (av. 0.5 mm. dia.) grains. The large porphyroclasts are strained. Scapolite is abundant and occurs as in specimen L1-81. The clinopyroxene is often rimmed by hornblende and/or hornblende-quartz inter-

(sausseritization?) at interfaces and along cracks and cleavages.

Ll-354: Foliated Epidote-bearing Facies

Ll-354 has a subophitic to granitic texture and shows complete recrystallization of plagioclase (An_{55}). Scapolite again engulfs considerable areas of plagioclase. The originally interstitial (?) clinopyroxene has been strongly uralitised with the growth of marginal hornblende. Locally, uralitisation is complete, with an intergrowth of hornblende and quartz rimmed by hornblende and occasionally biotite. The plagioclase are badly altered, especially along interfaces and fractures. Foliation is not observed in thin section.

A short description of the three envelope rock samples analyzed follows. The sample locations are shown on Map 1, page 4. Samples Mum-2 and S-32 were collected by R. Mummery, sample WB-4 was collected by this author.

1. Mum-2 - amphibolite:

Estimated thin section mode:

45% plagioclase
40% hornblende
5% quartz
5% garnet
5% opaque oxides

The mafic minerals are lineated and the specimen has a generally granoblastic texture.

2. S-32 - gneiss:

Estimated thin section mode:

50% quartz
35% K-feldspar
10% plagioclase
2% biotite
2% opaque oxides
1% garnet

The thin section shows a granoblastic texture, but does not show a lineation - this is probably a quartzo-feldspathic band.

3. WB-4: - granite gneiss:

Estimated mode:

60% K-feldspar
15% plagioclase (An_{10})
10% quartz
10% hornblende
3% opaque oxides
2% biotite

The mafic minerals are concentrated in bands with quartz, giving the specimen a good foliation.

APPENDIX B

ANALYTICAL PROCEDURE

B-I. Samples

1. Crack the ampoule open well above the sample and transfer the sample to a 20-25 ml. teflon crucible.

2. Add the rare earth carrier solutions to the crucible, ensuring that the sample is completely wetted.

3. Add about 5 ml. concentrated HF and about 2 ml. 60% $HClO_4$ and evaporate on a sand bath under heat lamps to copious $HClO_4$ fumes.

4. Add about 2 ml. 0.5 M HCl and 1 ml. 60% $HClO_4$ and evaporate to incipient dryness to convert fluorides to perchlorates.

5. Transfer the residue to a 150 ml. glass beaker by washing with 0.5 M HCl. Add 10 ml. 0.5 M HCl and heat until solution clears.

6. Add concentrated NaOH solution in excess to precipitate rare earths as hydroxides (about 25 ml.).

7. Transfer solution and precipitate to a 50 ml. polycarbonate centrifuge tube.

8. Centrifuge and discard the supernatant. Wash with dilute NaOH.

9. Dissolve the hydroxides in about 10 ml. 6 M HCl. Add 5 ml. concentrated HF and 5 ml. NH_4F (10% solution) to precipitate the rare earth fluorides. Centrifuge and discard the supernatant and wash with dilute HF.

10. Dissolve the fluorides in about 5 ml. 2 M HCl saturated with boric acid. Heat in sand bath to hasten dissolution.

11. To precipitate the rare earth hydroxides add 1:1 NH_4OH in excess.

Centrifuge and decant. Wash with dilute NH_4OH.

12. Repeat the fluoride-hydroxide cycle 3 times (steps 9-11).

13. Dissolve the last hydroxide precipitate in 15 ml. 8.0 M HCl, transfer solution to a 125 ml. separatory funnel and shake for 2 minutes with 15 ml. tri-butyl phosphate (pre-equilibrated with 8.0 M HCl, see note 1).

14. Drain the HCl phase containing the rare earths into a 25 ml. volumetric flask. Add 8 ml. 8.0 M HCl to the tri-butyl phosphate fraction, shake for 2 minutes and again drain the HCl phase into the volumetric flask.

15. Add 8.0 M HCl to bring the volume to exactly 25 ml. and put aside for counting.

B-II. Standards

1. Carefully clean the outside of the standard ampoules with acetone and 0.5 M HCl.

2. Crack the ampoule open and place it in a 150 ml. beaker to which the two rare earth carrier solutions have been added.

3. Completely remove the rare earths from the inside of the ampoule by repeated washing with the carrier solution. Finally, wash the ampoule using 0.5 M HCl, monitor to ensure removal of all rare earth activity, and discard the ampoule.

4. Add about 20 ml. 0.5 M HCl and stir to equilibrate carriers and standard.

Note 1: Take 50 ml. portions of tri-butyl phosphate and shake overnight with about the same volume of 8.0 M HCl. Decant and store the tri-butyl phosphate.

5. Add concentrated NaOH solution in excess to precipitate rare earth as hydroxides.

6. Transfer solution and precipitate to a 50 ml. polycarbonate centrifuge tube, centrifuge and discard the supernatant. Wash once with dilute NaOH.

7. Dissolve the precipitate in about 15 ml. 8.0 M HCl and transfer to a 25 ml. volumetric flask. Add enough 8.0 M HCl to bring volume to 25.0 ml.

8. Shake the flask to obtain a homogeneous solution and put aside for counting.

B-III. Chemical Yields

Chemical yields are determined by re-irradiation of accurately weighed fractions of each sample and standard. The absolute yield is not determined - only the yield of REE in each sample relative to the yield in the standard is determined by the following method:

1. Accurately weigh about 0.1 ml. of each sample and standard into silica ampoules.

2. Evaporate the solutions to dryness in a heating oven (at 70-80 ^{o}C) and seal the open end of each ampoule by fusing.

3. Irradiate together the 6 sample and 1 standard ampoules for 5 minutes and cool 4 days.

4. After breaking open each ampoule, transfer the activity completely into separate 1 dram vials by repeated washings with 0.5 M HCl.

5. Count each vial on the Ge(Li) detector to determine ^{140}La and ^{175}Yb activity.

By comparing the areas of gamma peaks 490 KeV ^{140}La and 396 KeV

^{175}Yb, the yield of La and Yb in the sample fractions relative to the standard fractions is calculated. This is converted to yield in the samples by multiplying by the weights of standard fraction over the weight of sample fraction taken. A linear relationship between yield and atomic number is assumed and the yield of the other REE is calculated accordingly.

The relative yield of La varied from 110% to 90% while the relative yield of Yb was lower, ranging from 102% to 81%.